University of Alberta

Drawdown of floating particles in stirred tanks

by

Oscar Khazam

©

A thesis submitted to the Faculty of Graduate Studies and Research in partial fulfillment
of the requirements for the degree of Master of Science

in

Chemical Engineering

Department of Chemical and Materials Engineering

Edmonton, Alberta
Fall, 2007

Library and
Archives Canada

Bibliothèque et
Archives Canada

Published Heritage
Branch

Direction du
Patrimoine de l'édition

395 Wellington Street
Ottawa ON K1A 0N4
Canada

395, rue Wellington
Ottawa ON K1A 0N4
Canada

NOTICE:
The author has granted a non-exclusive license allowing Library and Archives Canada to reproduce, publish, archive, preserve, conserve, communicate to the public by telecommunication or on the Internet, loan, distribute and sell theses worldwide, for commercial or non-commercial purposes, in microform, paper, electronic and/or any other formats.

AVIS:
L'auteur a accordé une licence non exclusive permettant à la Bibliothèque et Archives Canada de reproduire, publier, archiver, sauvegarder, conserver, transmettre au public par télécommunication ou par l'Internet, prêter, distribuer et vendre des thèses partout dans le monde, à des fins commerciales ou autres, sur support microforme, papier, électronique et/ou autres formats.

The author retains copyright ownership and moral rights in this thesis. Neither the thesis nor substantial extracts from it may be printed or otherwise reproduced without the author's permission.

L'auteur conserve la propriété du droit d'auteur et des droits moraux qui protège cette thèse. Ni la thèse ni des extraits substantiels de celle-ci ne doivent être imprimés ou autrement reproduits sans son autorisation.

In compliance with the Canadian Privacy Act some supporting forms may have been removed from this thesis.

Conformément à la loi canadienne sur la protection de la vie privée, quelques formulaires secondaires ont été enlevés de cette thèse.

While these forms may be included in the document page count, their removal does not represent any loss of content from the thesis.

Bien que ces formulaires aient inclus dans la pagination, il n'y aura aucun contenu manquant.

Canada

Abstract

Agitated tanks are used in several industrial processes to achieve drawdown of floating solids in liquids. The design requirements for this process are not completely defined, and are currently limited to heuristics regarding the use of a surface vortex. The effect of type of impeller, particles, solids concentration, submergence, and baffle configuration on the minimum draw down speed (N_{jd}) and power input (P_{jd}) were investigated. The formation of a large central vortex at the surface presented a poor performance. Intensity of turbulence and mean velocity of the liquid were responsible for drawdown and distribution in the tank. Submergence and the pumping mode of the impeller were found to be the controlling parameters.

Based on experimental observations a new configuration is proposed and, better distribution of particles and reduction of N_{jd} and P_{jd}, for solids drawdown relative to conventional configurations was obtained. CFD was used to gain a better understanding and interpretation of experimental observations.

Acknowledgements

I would like to thank the many people and institutions that made possible the completion of this work.

In the first place, I am deeply grateful to my supervisor Suzanne Kresta, for her thoughtful guidance and sincere and expert advice. I would also like to thank her for making this project a very enjoyable experience and for the understanding and kindness beyond the project.

Special thanks to the Mixing Research group for their useful comments throughout my thesis and for making the office an awesome place to work. Shad you are the best. Also I would like to thank the Department of Chemical and Materials Engineering and its administrative staff for their active support during my program.

I owe a lifetime of gratitude to my parents, brother and sister, whose confidence in me has been unwavering and for being my example of life. Thank you for the moral support that kept me afloat.

To my friends and family in Venezuela, Canada, and many other countries, thanks so much for your trust and love.

I would finally like to thank Lightnin and NSERC for their financial support to this project.

Table of Contents

List of Tables

List of Figures

Nomenclature

A   Coss-sectional area perpendicular to the flow (m^2)

B_H Baffle height (m)

B_T Baffle thickness (m)

CD   Cloud depth (m)

C_D Drag coefficient (-)

CFD   Computational Fluid Dynamics

d_p Particle size (mm)

d_T Impeller blade thickness (m)

D   Impeller diameter (m)

EPS   Expandable polystyrene beads

Fb   Bouyance force (N)

F_D Drag force (N)

Fg   Gravitational force (N)

Fsurf   Surface tension force (N)

F_{tur} Turbulent force (N)

Fr_{JS} Froud number at N_{js}(-)

g   gravity acceleration (m/s^2)

H   Liquid height in tank (m)

k   Turbulent kinetic energy per unit mass (m^2/s^2)

MRF   Multiple reference frames

N   Impeller speed (rps or rpm)

N_{jd} Just drawdown impeller speed (rps or rpm)

N_{js} Just suspended impeller speed (rps or rpm)

N_P Power number of impeller (-)

P   Impeller power consumption (W)

PBTD   Down-pumping pitched blade turbine

PBTU   Up-pumping pitched blade turbine

PE   Polyethylene grids

Re_I	Impeller Reynolds number (-)
S	Distance from the surface to the center of the impeller (m)
SG	Specific gravity (-)
T	Tank diameter (m)
Te	Temperature (°C)
$\overline{V}$	Velocity of the body relative to the medium (m/s)
V'	Velocity fluctuation of the critical eddy (m/s)
V_r	Radial velocity (m/s)
V_{sphere}	Volume of a sphere (m^3)
V_{sub}	Volume submerged of a sphere at the surface (m^3)
W	Baffle width (m)
w	Impeller blade width (m)
z	Vertical distance from the tank bottom (m)

Greek Symbols:

ε	Local rate of dissipation of turbulent kinetic energy per unit mass at any location (m^2/s^3)
ρ_B	Bayol density (kg/m^3)
ρ_L	Liquid density (kg/m^3)
ρ_S	Solid density (kg/m^3)
ρ_W	Tap water density (kg/m^3)
$\Delta\rho$	Density difference, $\rho_L - \rho_S$ (kg/m^3)
σ	Surface tension of fluid (N/m)
μ	Dynamic viscosity (kg/m-s)
ν	Kinematic viscosity, m^2/s

Chapter 1

Introduction

Industrial processes like water treatment, fermentation, and polymer processing require mixing operations. One of these operations involves the drawdown of floating solids. Identifying the mixing problems and finding efficient solutions to these problems is therefore an important part of the optimal design and operation of mixing equipment.

As described by Paul et al. (2003), a conventional stirred tank consists of a vessel equipped with a rotating mixer. The vessel is generally a vertical cylindrical tank. Non-standard vessels may have a square or rectangular cross-section. Horizontal cylindrical vessels are also sometimes used. The conventional tank employs a flat or dished bottom although other types are also available. The rotating mixer has several components: an impeller, shaft, shaft seal, gearbox and motor drive. Normally, for liquid height (H) between 30% and 120% of the tank diameter (T), only one impeller is used. The impeller rotates (usually clockwise from above) within the liquid and imparts angular momentum to it. In the presence of the baffles, the circumferential motion of the fluid is transformed into axial circulation. There are hundreds of impeller types in commercial use. Determination of the most effective impeller should be based on the understanding of process requirements and knowledge of physical properties.

Impellers can be grouped as turbines for low to medium viscosities and close-clearance impellers for high viscosity fluids. There are four types of turbine impellers, which are characterized by the flow patterns and level of shear they create: axial flow, radial flow, hydrofoil, and high shear impellers (Paul et al., 2003). However, a pitched blade turbine (PBT), which is one of the impellers of interest in the present study, is considered to be a mixed-flow impeller. The flow discharge of a PBT has components of both axial and radial flow velocity in low to medium viscosity liquids. A pitched blade turbine consists of a hub with an even number of blades. The blades can be at any angle between 10° and

1

90° from the horizontal, but the most common blade angle is 45°. Initially, the down-pumping pitched blade turbine (PBTD) was used for many applications where the flow needed to be directed toward the bottom of the tank. However, as described by Nienow and Bujalski (2004), the up-pumping PBTs have found use in increasing areas of operation covering numerous other applications.

Wall baffles are generally installed in stirred tanks for transitional and turbulent mixing to prevent solid body rotation (sometimes called "fluid swirl"). They typically consist of rectangular metal plates positioned in the path of tangential flows generated by the rotating impeller. Wall baffling has a significant influence on the flow behavior and resulting mixing quality. In the absence of baffles, the flow created by the impeller is two dimensional and causes swirling action (Kresta, 1991). Wall baffles transform tangential flows in vertical flows, provide top-to-bottom mixing without swirl, and minimize surface vortexing and air entrainment. Baffles increase the drag and power draw of the impeller. The standard baffle configuration (usually called "fully baffled") consists of four vertical wall baffles, although the actual number can be more or less depending on the process requirements. The baffle width (W) is 8 to 10% (T/12 or T/10) of the tank diameter.

The power draw is an important design parameter for a stirred tank and like many other characteristics of the flow, it depends strongly on the regime of operation. The operating regimes, fully turbulent, laminar or transitional, are demarcated by the Reynolds number. In a stirred tank, the flow is driven by the impeller, and the proper characteristic length and velocity scales are the impeller diameter (D) and the tip speed of the impeller (πND). The Reynolds number for agitation (or simply the impeller Reynolds number) is thus:

$$\text{Re}_I = \frac{\rho ND^2}{\mu}$$

(1)

When Re_I is less than 10, the flow is completely laminar. The flow is fully turbulent for $\text{Re}_I \geq 2\text{x}10^4$ (Paul et al., 2003). Apart from the Reynolds number, there are two other

2

dimensionless numbers commonly used to characterize the hydrodynamic condition of an impeller, one related to its power consumption and the other to the flow generated by it. The power consumption is related to N and D by the following expression:

$$P = Np \cdot \rho \cdot N^3 \cdot D^5 \qquad (2)$$

The equation above can also be obtained from an angular momentum balance across the impeller if the three-dimensional flow field is accurately known in the suction and the discharge sides of the impeller (Chapple and Kresta, 2002). Np, called the power number, is a proportionality constant dependent on the impeller type and in general also on Re_I.

Mechanically agitated vessels are widely used in the chemical processes in industries for a variety of process objectives: one of which is the drawdown of floating solids. In this process, the goal is to obtain a complete distribution of solids to promote the maximum contact between the solid and liquid phases. This problem can be approached by dividing it into two objectives: first finding the optimal mode of drawing down the floating particles and second being able to distribute the particles evenly within the tank. Particles may float on a liquid surface due to a density difference, due to low wettability combined with a large contact area, or due to low bulk density of the solid powder. Accumulation of solids at any point in the system is often observed and can be problematic, but clumping of sticky solids was not directly addressed in this work.

If a single particle is dropped at the surface of a stationary denser and/or non-wetting liquid, as shown in Figure 1.1, the buoyancy (F_B) and surface tension (F_{surf}) forces are greater than the gravitational force (F_g) and the particle stays at the surface. The three forces expressions are:

$$F_B = \rho_L \cdot g \cdot V_{sub} \qquad (3)$$

$$F_{surf} = \sigma \cdot c \qquad (4)$$

$$F_g = \rho_S \cdot g \cdot V_{sphere} \qquad (5)$$

Where c is the wetted perimeter of the particle.

3

Two additional forces, the drag force and the turbulent force, emerge in the system once energy is supplied by the action of the impeller. The two forces expressions are:

$$F_D = C_D \cdot \rho_L \cdot A \cdot \frac{\overline{V}^2}{2} \qquad (6)$$

$$F_{tur} \; \alpha \; \rho_L \cdot d_p^{\;2} \cdot V'^2 \qquad (7)$$

These forces and the gravitational force have to overcome the buoyancy and surface tension forces to submerge the floating particles and distribute them throughout the tank.
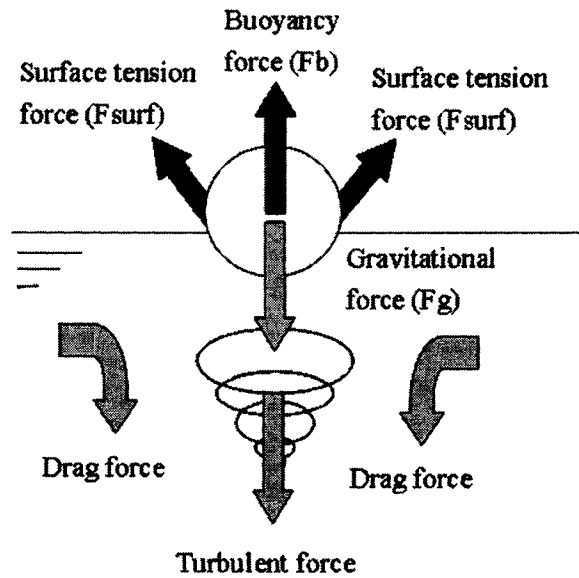
Figure 1.1: Forces that interact once a buoyant particle is placed at the surface of a denser liquid. Note that the drag force is determined by the axial component of the mean velocity.

When working with floating particles, one might expect to begin by drawing an analogy between off-bottom suspension and solids drawdown. However, close observations and experiments reveal quite different mechanisms. This is discussed further in Chapter 2. Previous research has established design rules for two phase systems (Nienow, 1968; Baldi et al., 1978; Rao et al., 1988; Mak, 1992; Choudhury, 1997), where the solids are denser than the liquid phase and the Zwietering (1958) correlation can be used to calculate the just suspended speed, N_{js} (Paul et al., 2003). In several industrial

4

applications the solids are less dense than the liquids and solids drawdown is required to produce a well dispersed suspension.

The drawdown of floating solids in a mixing vessel is a research area that has been given very little attention in the literature (Joosten et al., 1977; Hemrajani et al., 1988; Thring et al., 1990; Özcan-Taskin et al., 2001; Özcan-Taskin et al., 2003), despite the importance of this problem in industrial processes. The type and size of impeller, particle size and shape, solids concentration, impeller submergence, and baffle configuration all affect solids drawdown. A good understanding of the interactions between these variables and their effect on the minimum drawdown speed and power input is needed to obtain a useful solution for floating solids systems.

The paper on solids drawdown by Joosten et al. (1977) correlated the minimum drawdown speed by

$$Fr_{JS} = 3.6 \times 10^{-2} \cdot \left(\frac{D}{T}\right)^{-3.65} \left(\frac{\Delta\rho}{\rho_L}\right)^{0.42} \tag{8}$$

They used a single partial baffle 0.2T wide, immersed from the top of the liquid to a depth of 0.3T, an axial impeller of 0.6T diameter, and the impeller blade height in the range of (1/9-3/9)T as the optimum configuration. In this configuration, an eccentric surface vortex draws the solids down to the impeller.

Later work by Hemrajani and co-workers (1988) observed a two-step process in unbaffled tanks. In the first step the centrifugal forces resulting from the swirl moved the light particles along the liquid surface into the center of the vortex. There the liquid velocities at the surface at this central location were high enough to incorporate the particles into the bulk liquid.

Bakker and Frijlink (1989) used three different types of impeller, a six bladed disc turbine and two inclined blade impellers with 45° and 60° blade angle and six blades. The latter were used in down- and up-pumping modes. All the impellers had a diameter of D=0.4T. They found that the 45° up-pumping impeller is the most energy efficient as a

5

result of the low speed and power number obtained. However, the particles tended to concentrate in the upper half of the vessel and the suspension was not homogeneous in all cases.

In a fully baffled tank, the intensity of turbulence is primarily responsible for the dispersion of floating solids as report by Kuzmanic et al. (2001). They also concluded that with an increase in impeller diameter, less decay in the turbulence will occur because of the reduction of flow path length from the impeller to the surface. Moreover, the liquid velocity increases with an increase in impeller diameter. These two overall effects lead to a significant dependence on impeller diameter.

Previous investigations (Özcan-Taskin et al., 2001; Takahashi et al., 1999; Thring, 1990; Joosten et al., 1977) showed that substantial savings can be achieved by choosing the proper impeller type and size. All conclude that radial flow impellers are not energy efficient for drawing down solids. They also report that mixed flow impellers achieve better results than the axial flow impellers, although the performance of the mixed flow impellers is still not well defined when they are compared based on the pumping mode of the impeller (up- or down-pumping).

Özcan-Taskin et al.,(2001) suggests that prevention of air or vapour entrainment from the headspace may be required to ensure the desired product quantity. Slurry homogeneity, rate of drawdown and fouling on vessel internals can be additional constraints for design and operation of solids drawdown. In a later study, Özcan-Taskin and Wei (2003) observed that solids are drawn down in different ways depending on the impeller pumping mode, submergence, and number of baffles. They worked with a pitched blade turbine (PBT) in the up- and down-pumping modes and the LE-20 impeller in the up-pumping mode. All three impellers were studied for D = T/2 and D = T/3. Four different submergences were used (S = T/3, S = T/2, S = 2T/3 and S = 3T/4). The conclusion of their work is that for most cases decreasing the impeller submergence increases the speed and power required to drawdown the solids. The opposite behavior was observed when a down-pumping impeller with D = T/3 was used: a larger submergence was more effective.

6

In a study of large tanks (H/T ratio higher than 1.5) down-pumping impellers performed better than up-pumping impellers (Siddiqui, 1993). According to this work a better homogenization in the slurry was achieved by running three down-pumping impellers in a H/T = 3 tank. Also in these experiments 45° PBTs were operated at 300 rpm in comparison with 760 rpm when three A100 impellers were used to achieve equivalent solids dispersion. Therefore, the use of a PBT impeller seems to be one of the most efficient impellers for drawing down floating solids.

This study considers the effect of the impeller size and pumping mode, solids concentration, impeller submergence, and baffle configuration on the minimum drawdown speed (N_{jd}) and the dominant solids drawdown mechanism. The drawdown mechanisms that were identified during the experiments are defined in Chapter 2. In addition, Chapter 2 shows the comparison in between the three impellers studied using three conventional baffle configurations. They are compared in terms of N_{jd} and cloud depth. The fully baffled PBTD configuration is used to study the effects of solids density, surface tension and particle wetted perimeter on solids drawdown behavior.

Chapter 3 evaluates the two new baffle configurations based on the mechanisms identified in Chapter 2. Four half-baffles at the top of the tank and the four surface baffles were compared with the fully baffled configuration in terms of N_{jd} and cloud depth (CD). The PBTD and PBTU impellers are compared with each other to see the influence of impeller diameter and pumping mode. Lastly, the effect of the fully baffled and surface configurations on the power number (Np) and power draw at N_{jd} is measured.

Chapter 4 summarizes the main ideas and highlights the key results obtained in this study of the drawdown of floating solids in stirred tanks.

7

Chapter 2

Drawdown Mechanisms

In this work, the drawdown of floating solids is divided in three objectives: the initial objective was to observe the behavior of the system using different conventional baffle configurations. Three dominant mechanisms for solids drawdown at the surface were identified from these observations, satisfying a more general second objective which is to gain a more fundamental understanding of the process. Impeller selection is an important step in choosing the best mixing configuration. Hence, a third objective of this study considers the effect of impeller type in terms of impeller submergence. Both the up- and down-pumping PBTs and the A340 impellers are evaluated based on the dominant solids drawdown mechanism and values of N_{jd} and cloud depth for each impeller. Computational Fluid Dynamics (CFD) simulations were carried out to obtain a better understanding and interpretation of the flow patterns and drawdown mechanisms for the fully baffled configuration. Finally, from the mechanisms identified, larger values of N_{jd} are expected for larger density differences, and a large wetted perimeter will also require an increased N_{jd}. Results are presented for four different solids in two different liquids to quantify theses effects.

2.1 Drawdown Mechanisms

Observations of the liquid surface from above and through the side of the vessel revealed that solids may be drawn down through three different mechanisms:

2.1.1 Single vortex formation: this mechanism is characterized by a large vortex which usually forms in the center of the tank when no baffles are present. This vortex breaks up the stagnant zones at the surface, but the solids are not distributed throughout the tank. They collect on the surface of the vortex, where they spin around to finally accumulate at

8

the center by centrifugal forces. The mean velocity is primarily tangential throughout the tank for this mechanism. The size of the vortex depends on the type of impeller and the submergence. A variant on this mechanism is the off-center vortex which forms for the single baffle configuration.

2.1.2 Turbulent fluctuations: this mechanism is characterized by a wavy and splashy surface with energetic surface eddies. Small eddies form around the shaft when the down-pumping impeller and a small submergence are used. These eddies help drawdown of particles, but they are not constant and they appear and vanish quickly. In addition, if these eddies are smaller in scale then the particles, they do not have the energy necessary to drawdown the particles.

2.1.3 Mean drag: this mechanism is characterized by large swirls and waves which develop over the entire free liquid surface, breaking up the stagnant zones intermittently and ingesting more solids. A better distribution of particles in the tank is achieved in comparison with the single vortex formation mechanism. The mean component of the velocity must be primarily axial at some point close to the liquid surface for this mechanism to be effective.

It is important to mention that combinations of these mechanisms can be found in any tank configuration, but one mechanism will generally dominate. As an example, the one baffle configuration is characterized by a big unstable vortex shifted from the center of the tank. The single vortex formation mechanism dominates. This configuration is more efficient in drawing down and distributing the solid particles relative to the unbaffled configuration. As a result of the centrifugal forces from the swirl, the particles are moved along the liquid surface from the walls of the tank into the center of the vortex. The mean drag and top to bottom circulation induced by the single baffle is usually high enough to incorporate these particles into the bulk of the liquid.

9

2.2 Experimental

Experiments were performed in a 0.24m diameter flat bottom transparent cylindrical tank that has a provision to add or remove baffles and to change the baffle configuration. Tap water (ρ_W = 998 kg/m^3) and Bayol (ρ_B = 794 kg/m^3) were used as the working fluids. The liquid height was maintained constant (H = T = 0.24m) in all the configurations used in this work. A schematic diagram of the experimental apparatus is given in Figure 2.1.
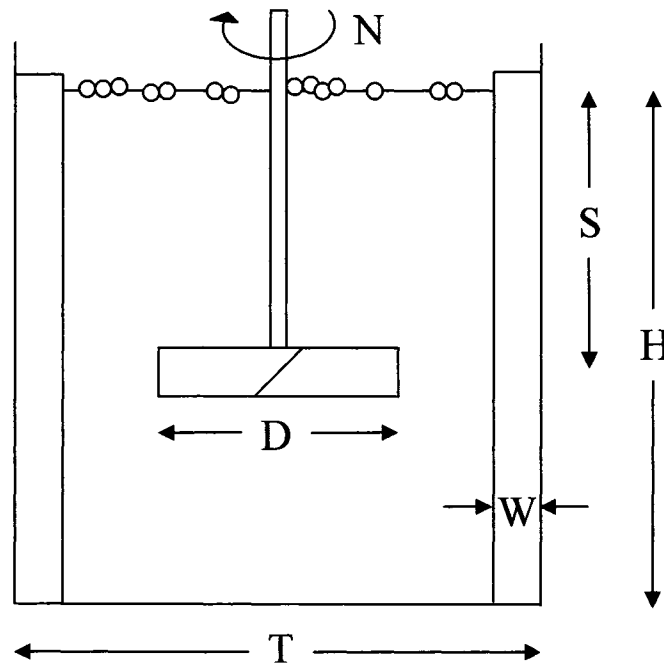
Figure 2.1: Schematic diagram of the experimental apparatus with a PBTU

A variable-speed motor (80-600 rpm) supplied the necessary power to the system. The distance from the surface of the liquid to the middle of the impeller (submergence, S) was varied from the impeller blade height to half of the liquid depth (0.01m < S < 0.12m). Three impellers were used: a standard 45° pitched four-blade turbine (PBT) used in both up and down-pumping modes, and an A340 impeller (Lightnin). See Table 2.1 for impeller specifications.

10

Table 2.1: Impeller specifications

	PBT	A340
Impeller		
Diameter	D = T/2 &T/3	D = 4T/9
Pumping mode	Down and up	Up
Blade width, w	D/5	4D/9
Blade thickness, d_T	D/60	D/60

Three standard baffle configurations were used and all of the baffles had the same dimensions: baffle width (W = T/10), baffle height (B_H = 1.1T) and baffle thickness (B_T = T/120). Configurations with zero, one and four baffles were examined. Four particle species were used in the experiments: three different expansions of polystyrene beads (EPS) and polyethylene grids (PE). The EPS beads were used to compare the effect of reducing solids density, and the PE grids were used to test the effect of contact area with a neutrally buoyant particle. The EPS beads were prepared from unexpanded samples by holding them under hot water (Te ≈ 70°C) until no particles remained on the bottom of the beaker. After expansion, the particles were sieved to separate them by size and their density was measured using a pygnometer. All of the particles are partially-wetting in water, and fully wetting in Bayol. Only the EPS2 and EPS3 particles floated in Bayol. Particle specifications are as follows:

Table 2.2: Particle specifications

Particle	Specific gravity (S.G)	Particle size (d_p)
Expandable Polystyrene beads (EPS 1)	0.9	1mm
Expandable Polystyrene beads (EPS 2)	0.4	1.5mm
Expandable Polystyrene beads (EPS 3)	0.3	2mm
Polyethylene Grids (PE)	1	~8mm x 8mm

11

For every series of experiments, the EPS beads and the PE grids were weighed and gently dropped down the side of the tank with the impeller turned off. Next a small impeller speed was set giving stagnant zones where a number of particles agglomerated at the surface (Figure 2.2a). Then the speed of the impeller was gradually increased at intervals of 5 rpm until no solids remained at the liquid surface for more than 1 to 2 seconds. This speed was characterized as N_{jd}. The velocity was taken from the digital display of the variable-speed motor, and checked with a hand-held electronic tachometer. At N_{jd}, the just drawdown speed, the stagnant zones of solids completely broke up and all the solids were drawn down into the liquid. This criterion was used for all the experiments. It was difficult to determine this point exactly and objectively because even at higher impeller speeds some solid particles reappeared on the liquid surface (Figure 2.2b). To minimize the uncertainty in N_{jd}, each value of N_{jd} was obtained from three different runs and averaged.

(a)   (b)
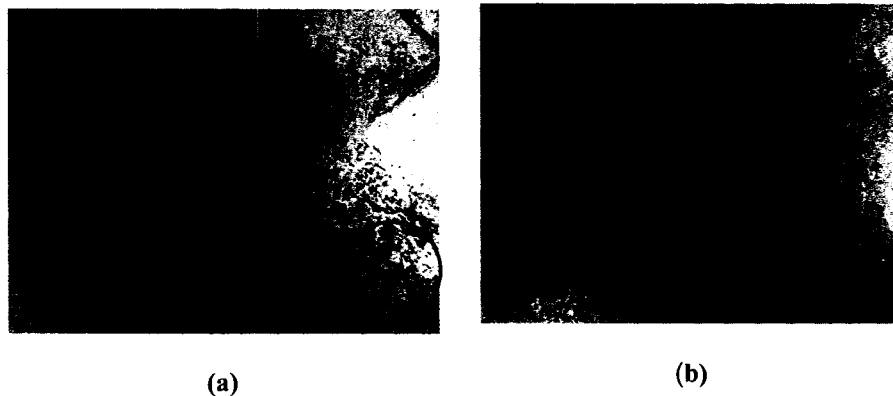
**Figure 2.2: Surface view of the solid-liquid system (PBTD, S = T/3, 4 full baffles configuration): a. N = 270 rpm with clusters of particles remaining on the surface.
b. N_{jd} = 295 rpm.**

The cloud depth, which is the perpendicular distance from the lowest point on the free surface of the liquid to the point where the concentration of particles drops dramatically, was also measured for each configuration. An illustration of the cloud depth for the unbaffled configuration is shown in Figure 2.3. While N_{jd} gives the point where all of the particles leave the surface, and allows both design and motor sizing, the cloud depth gives an indication of how well the particles are dispersed throughout the tank. The cloud

12

depth reported here is a subjective measure of the drop in concentration. For some configurations, the solids layer is very compressed and the CD measurement is straightforward. For other configurations, the concentration of solids changes in several stages, and the CD reported is the point beyond which very few particles penetrate. No direct measurement of concentration was available for this study, and the CD was simply measured using a ruler, and averaged over three runs. The results are accurate to approximately 0.1T.
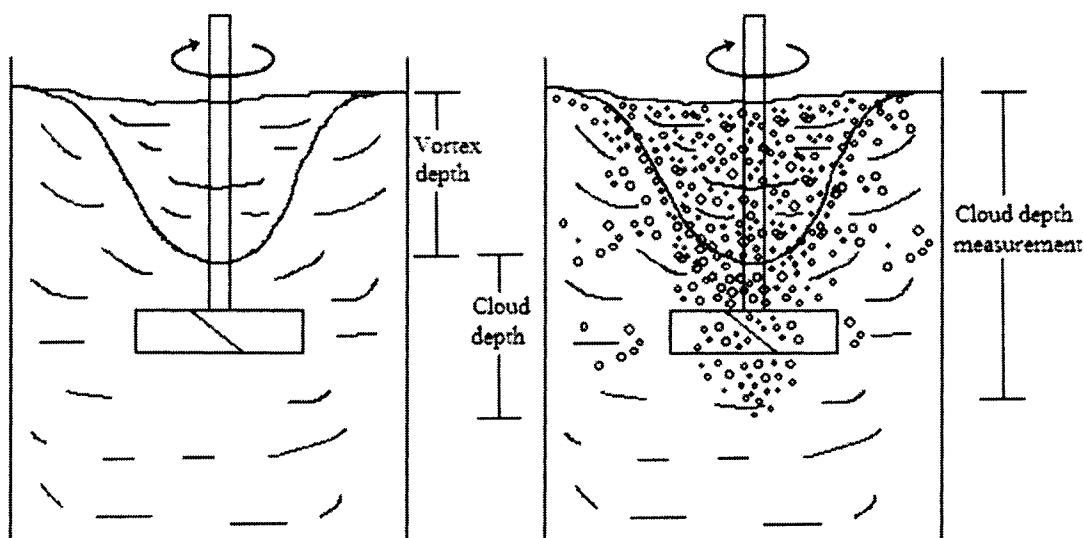
Figure 2.3: Sketch of cloud depth in solids drawdown systems for the unbaffled configuration.

2.3 CFD protocol

Many papers have been published on the CFD simulation of flow in stirred tanks, and several conclusions may be drawn about the accuracy of these simulations:

1. The recirculation flow produces a strong coupling of momentum exchange between the impeller and the tank geometry, so the impeller must be simulated directly (Fokema et al., 1994).

13

2. Predicted circulation patterns are always qualitatively accurate, and the transitions from one circulation pattern to another, predominantly with changes in off bottom clearance, are also accurately predicted (Fokema et al., 1994, Coy et al., 1996).

3. Turbulence and flow are typically under-predicted in the bulk of the tank, primarily because the k-ε model is over diffusive for round jets (Bhattacharya and Kresta, 2002). LES promises more accurate simulation of the turbulence, but simulation times are still very long (one month for LES/SGS model vs one hour for MRF/k-ε).

4. Small concentrations of a second phase do not significantly affect overall circulation patterns, but the meaning of "small" in this context is not well established (Montante et al., 2001).

Simulations were used in this project to explore large changes and trends in the mean flow and turbulence near the surface of the tank. This allowed us to confirm visual observations from the laboratory and thus provide a better understanding of the dominant mechanisms for various geometries. With these observations in place, a direction for future investigations can be established, and it is our intent that these results serve to guide later researchers in the design of experiments to further explore the detailed fluid mechanics associated with drawdown of floating solids. With this limited objective for the CFD simulations in mind, several gross assumptions were made:

1. Single phase simulations will show the same trends for gross changes in mean flow and turbulence as exist in the flow field with solids present. Experiments were performed to establish the effect of solids concentration on the results, and it will be shown later that the trends observed are independent of solids concentration, which lends support to this difficult assumption.

14

2. The distortion of the free surface for the fully baffled (4 full height baffles) is negligible in terms of its effect on the simulations. Accurate prediction of surface turbulence and the medium scale transient eddies observed for the single baffle case would require a more accurate treatment of the free surface, but for the fully baffled case this approximation is reasonable.

3. The Multiple Reference Frames (MRF) protocol defined by Bhattacharya and Kresta (2002) is suitable for the PBTU as well as the PBTD. The full details of the protocol development are given in Bhattacharya and Kresta (2002).

Simulations were carried out using the Multiple Reference Frames (MRF) formulation, where a rotating volume is associated with the impeller and a stationary zone is associated with the baffles and the tank wall. The surface was modeled as a symmetry plane (zero velocity gradients) and no-slip boundary conditions were used for the tank wall, impeller, shaft, and baffles. In these simulations, the MRF boundary was placed at two thirds of the way to the wall. Iterations were continued until the normalized residuals of all the variables were less than 2×10^{-5}.

The effect of impeller submergence on the velocity fields was studied for S = T/4 and S = T/2. The simulations were carried out at the respective N_{jd} values for each of the configurations of interest using a T = 0.24m impeller and the fully baffled configuration. Water was used as the working fluid in all cases ($\rho = 1000$ kg/m^3 and $\mu = 0.001$ kg/m·s). Full details of the four geometries are given in Table 2.3

Table 2.3: Four geometries simulated using CFD

Configuration	1	2	3	4
Impeller type	PBTD	PBTD	PBTU	PBTU
Impeller diameter	D = T/2	D = T/2	D = T/2	D = T/2
Submergence	T/2	T/4	T/2	T/4
N_{jd}(rpm)	350	280	400	230

15

The tank geometry, impeller type, impeller dimensions (shaft diameter, hub size, blade width and thickness) and the rotational speed were set using MixSim version 1.7, a mesh generator which creates a structured grid. The grid resolution is 60 hexahedral cells per tank diameter, which gave around a million cells per tank. Subsequently, the CFD calculations were launched in FLUENT version 4.2.16 using the k-ε turbulence model. The conditions used here are summarized in Table 2.4.

Table 2.4: CFD simulation protocol

Commercial code	Fluent 4.2.16
Flow Equations	Navier Stokes equations
Turbulence Model	k-ε model with standard constants
Other Model Equations	none
Impeller Model	MRF with full impeller geometry; boundary placed at 2/3 of the tank radius
Grid Generator	MixSim 1.7; hexahedral mesh
Grid Resolution	1 million cells total 60 cells across the tank diameter
Numerical Scheme	Second order discretization by the Segregated Solution Method
Convergence Criterion	all normalized residuals $< 2 \times 10^{-5}$
Boundary Conditions	see text
Working Fluid	water, $v=1\times10^{-6}m^2/s$; $\rho=1000$ kg/m^3

2.4 Results and Discussion

Determining the effect of baffle configuration on drawdown of floating solids was one of our main objectives. Figure 2.4 provides an overview of what was observed in the form of pictures and sketches of the different baffle configurations and the associated solids

16

distributions and flow patterns. The unbaffled and one-baffle configuration pictures clearly show the single vortex formation mechanism and how poor the distribution of particles is throughout the tank in these cases. Most of the particles for these two configurations accumulate at the surface of the vortex. On the other hand, the picture of the fully baffled configuration shows good solids distribution and the absence of a single stable surface vortex. The solids distribution is similar for both the PBTU and the PBTD, but the flow patterns are quite different. The key difference between the four full baffles and the partially baffled or unbaffled cases is the top to bottom circulation, and the elimination of the surface vortex. The drawdown mechanisms defined before and partially illustrated in Figure 2.4 clearly show that the best way to drawdown floating particles is to avoid the formation of a big vortex and to create turbulence and strong mean circulation at the surface. These characteristics are seen in the fully baffled configuration, where the baffles suppress the vortex formation and produce a strong top-to-bottom circulation in the bulk of the tank. CFD simulations of the fully baffled configuration were carried out to verify and support the visual observations and N_{jd} results.

Figure 2.5 shows the flow field for two submergences of the PBTD, both at N_{jd}. From these results we can see the direction and magnitude of the flow created by the impeller and the size of the different recirculation loops present. The mean circulation drags the particles from the surface and then distributes them throughout the tank. The direction and magnitude of the velocity arrows at the surface suggest that the particles are carried from the walls and then immersed around the shaft for both submergences of the PBTD. The velocity vectors at the surface are much smaller for S=T/2 (Figure 2.5a) even though N_{jd} is larger than for the S=T/4 configuration (Figure 2.5b), suggesting that turbulence at the surface will be a more important mechanism than mean drag as S increases.

17

Baffle configuration	Top view of the tank	Sketch of the system	Experimental picture
No baffles (unbaffled)			
One baffle			
Fully baffled: Four full baffles (PBTD and (PBTU)		Down-pumping Up-pumping	
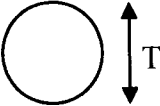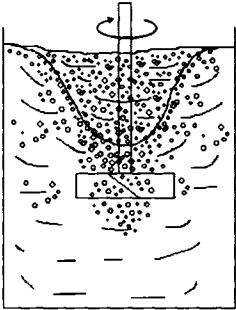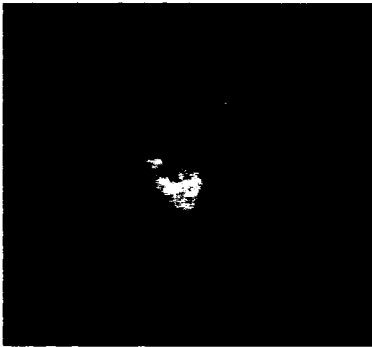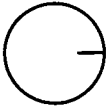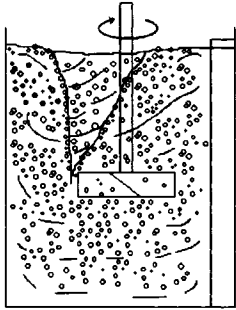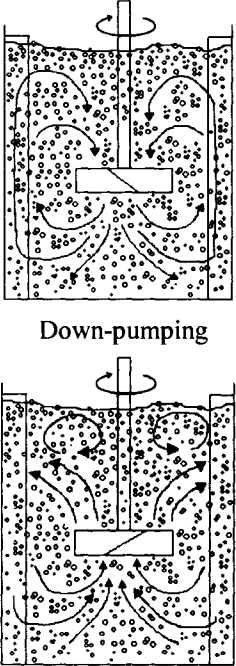
Figure 2.4: Different baffle configurations studied.

18
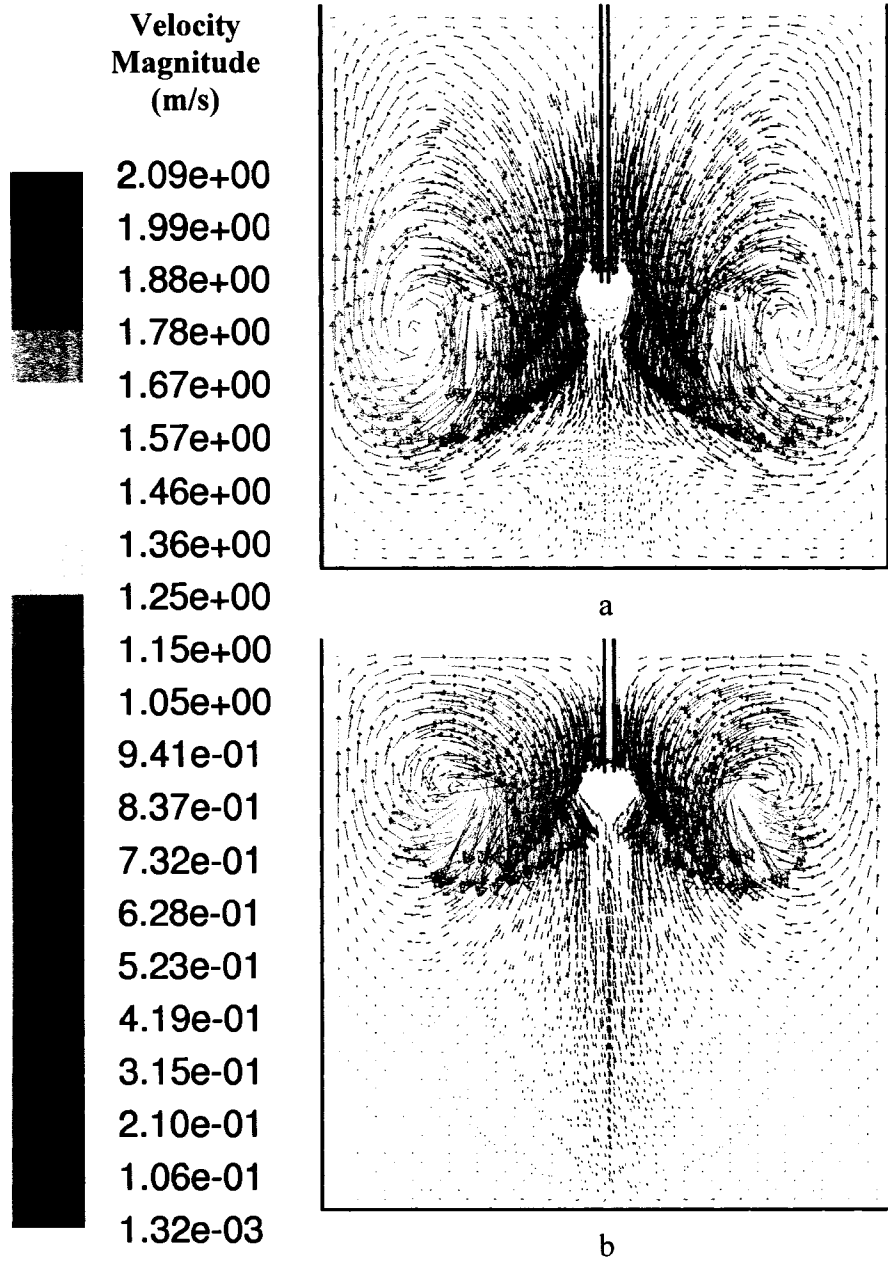
Figure 2.5: CFD simulation results for the four full baffles with the PBTD. Velocity vectors in the mid-baffle plane at N_{jd} are shown for the following configurations: a. S = T/2, N_{jd} = 350rpm. b. S = T/4, N_{jd} = 280rpm.

Figure 2.6 shows experimental results for N_{jd} for the down-pumping impeller, PBTD, for all three baffle configurations. For very small submergences, the drawdown is dominated by turbulence at the surface and N_{jd} is quite small. As the impeller moves away from the surface a greater liquid circulation velocity is needed to achieve complete drawdown of the floating solids and the dominant mechanism shifts to drag on the particles induced by

19

mean circulation. From 0.25< S/T< 0.4, both mechanisms are active and N_{jd} is nearly constant. A second increase is observed beyond S/T=0.4. This behavior can be explained in the context of the intensity of the recirculation loops driven by the impeller and the intensity of turbulence at the surface. Once the distance between the impeller and the liquid surface exceeds S/T=0.3, the wall jet which drives the up-flow in the recirculation loop disintegrates at z/T=0.7 so the mean flow and turbulence no longer penetrate to the surface (Bhattacharya and Kresta, 2002). The just drawdown speed increases as a result.
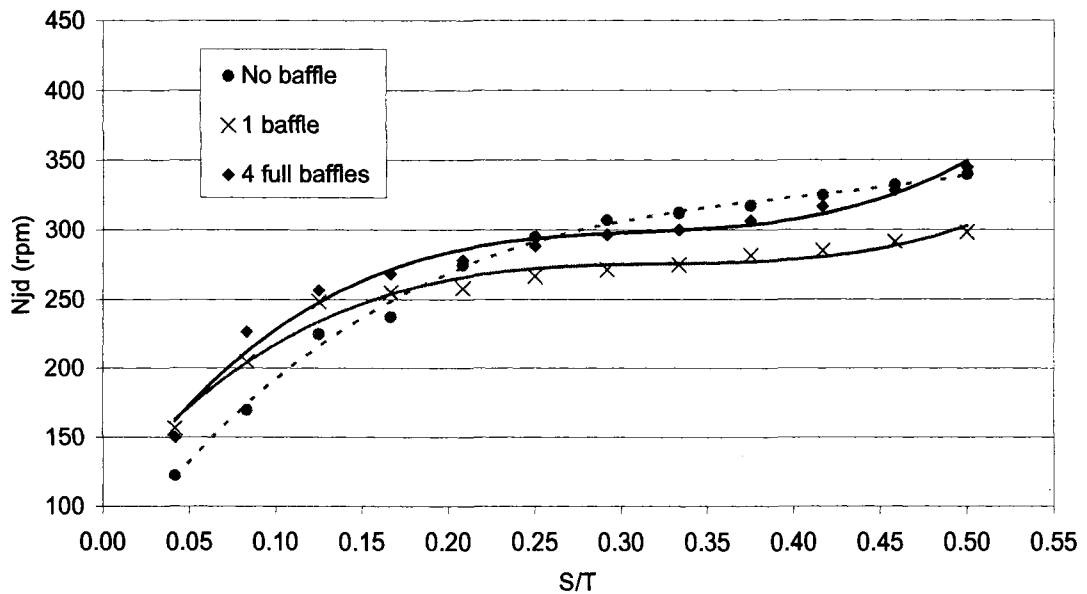
Figure 2.6: Effect of baffle configuration on N_{jd} for the PBTD (D = T/2, 2%v/v). Note that for unbaffled configuration, the particles are submerged but not dispersed as illustrated in Figure 2.4.

Since we are interested in both pulling the solids down from the surface, and in distributing them throughout the tank, the cloud depth was also measured. The cloud depth is the perpendicular distance from the surface of the liquid to the point where the concentration of particles drops dramatically, and is an indication of how the particles are distributed throughout the tank. It is analogous to the cloud height for solids suspension. For the unbaffled configuration, the cloud depth was calculated by subtracting the vortex depth without particles from the vortex depth to the bottom of the particle layer when particles are added.

20

Figure 2.7 shows the vortex depth at N_{jd} for all the impellers studied at varying impeller submergence. The A340 vortex depth is smaller even though N_{jd} is larger. Clearly, as the vortex depth increases, N_{jd} and the power requirement also increase. At the same time, we see that the cloud depth, or the quality of solids distribution, decreases as the submergence and vortex depth increase (Figure 2.8).
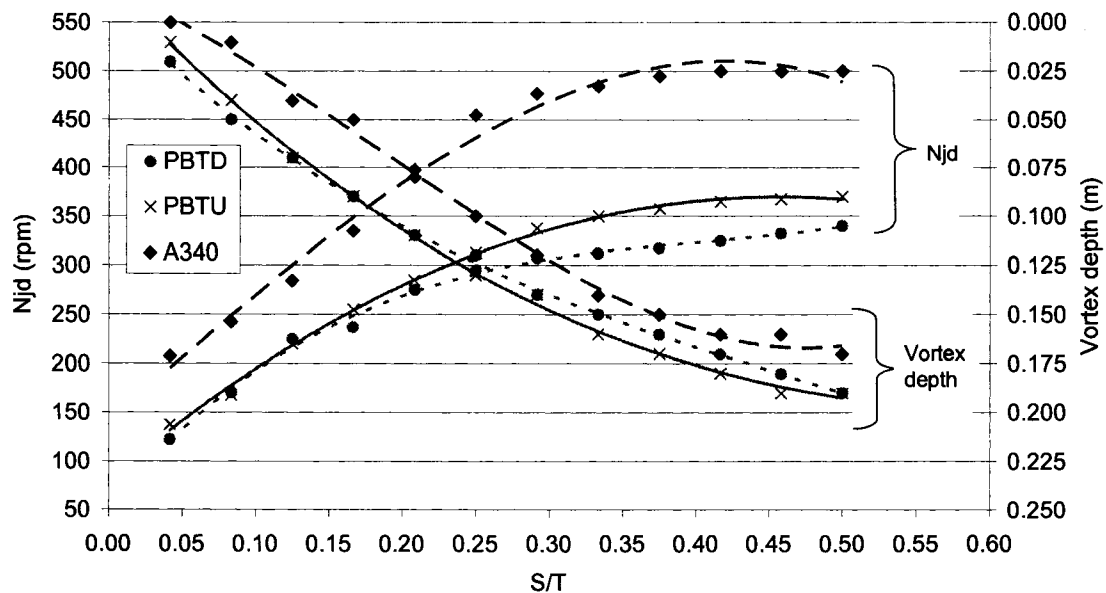
Figure 2.7: Effect of impeller type and submergence on the vortex depth and N_{jd} for the unbaffled configuration (PBTD and PBTU both with D=T/2 and A340 with D=4T/9).

Figure 2 shows that the thickness of the layer of particles in the single vortex formation for the unbaffled configuration decreases as S is increased and N_{jd} increases. This is because of the increasing size of the centrifugal forces associated with the rotational flow. In comparison with the other configurations studied, the performance of the unbaffled configuration is significantly poorer, because most of the particles accumulate near the vortex surface. With a light solid like the expandable polystyrene beads, the concentration of particles is not uniform in the tank even after large values of cloud depth are obtained.

21

For the fully baffled configuration and the single baffle configuration, the cloud depth varies with S/T. Referring back to Figure 2.5 for the fully baffled configuration, the top to bottom recirculation loop is larger when S/T=0.5 than when S/T=0.25. This indicates that the particles should be driven deeper in the tank for S/T=0.5, which agrees with the trends in Figure 2.8 for the fully baffled case. The results for the single baffle case fall between those for the surface vortex and the fully baffled case, as we might expect, but are much closer to the fully baffled case. This clearly illustrates the importance of top to bottom circulation for solids distribution throughout the tank. For the PBTD, there is little effect of S/T or baffle configuration on N_{jd}, but there is a dramatic difference in the cloud depth for the different configurations. The use of a surface vortex for solids drawdown is not effective, particularly for the distribution of particles throughout the tank.
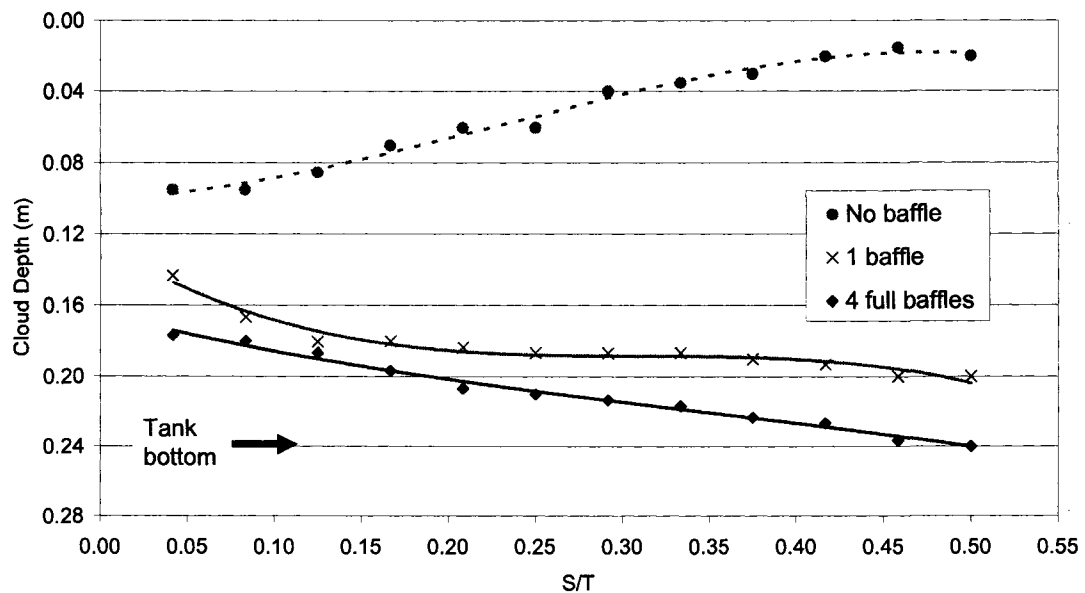
Figure 2.8: Cloud depth for the PBTD (D = T/2, 2%v/v). Note the poor performance of the unbaffled configuration. In this highly rotational flow, the particles are collected at the surface of the vortex due to centrifugal forces.

The results for the PBTU are quite different from those for the PBTD, as one might expect from the circulation patterns for the PBTU shown in Figure 2.9. Two recirculation loops are present in the system for S/T=0.5 (Figure 2.9a). The large intensity and magnitude of the velocity vectors in the main recirculation loop shows that almost all the

22

turbulent kinetic energy discharged by the impeller is dissipated there. For larger submergences, the discharge flow of the impeller hits the wall before it reaches the surface and a weak secondary circulation loop forms at the surface. In the upper circulation loop, the velocity is low and therefore the mixing is rather poor at the surface. This configuration locates most of the mixing action in the lower three quarters of the tank. Most of the turbulent kinetic energy discharged by the impeller is dissipated in the bulk, within the primary circulation loop, hardly reaching the surface.

When the up-pumping impeller is used with a small submergence, the flow at the surface is much stronger and the particles are swept from the surface to the walls, where a zone of rapid downward circulation is found. This downward flow occurs when the primary discharge flow from the up-pumping impeller reaches the surface before it reaches the sidewalls of the vessel (S/T<0.375).

Moving now to the N_{jd} results for the PBTU, shown in Figure 2.10, there is very little difference in the drawdown mechanisms between the unbaffled and one baffle configurations, but the four baffles configuration shows dramatically different behavior, particularly as the submergence is increased. As the submergence goes from 0.32 to 0.42, the N_{jd} increases dramatically. Referring to Figure 2.9, it is clear that this is the same region where the secondary circulation loop forms close to the surface, dramatically reducing the effectiveness of the PBTU.

23

Velocity Magnitude (m/s)

2.09e+00
1.99e+00
1.88e+00
1.78e+00
1.67e+00
1.57e+00
1.46e+00
1.36e+00
1.25e+00
1.15e+00
1.05e+00
9.41e-01
8.37e-01
7.32e-01
6.28e-01
5.23e-01
4.19e-01
3.15e-01
2.10e-01
1.06e-01
1.32e-03

a

b
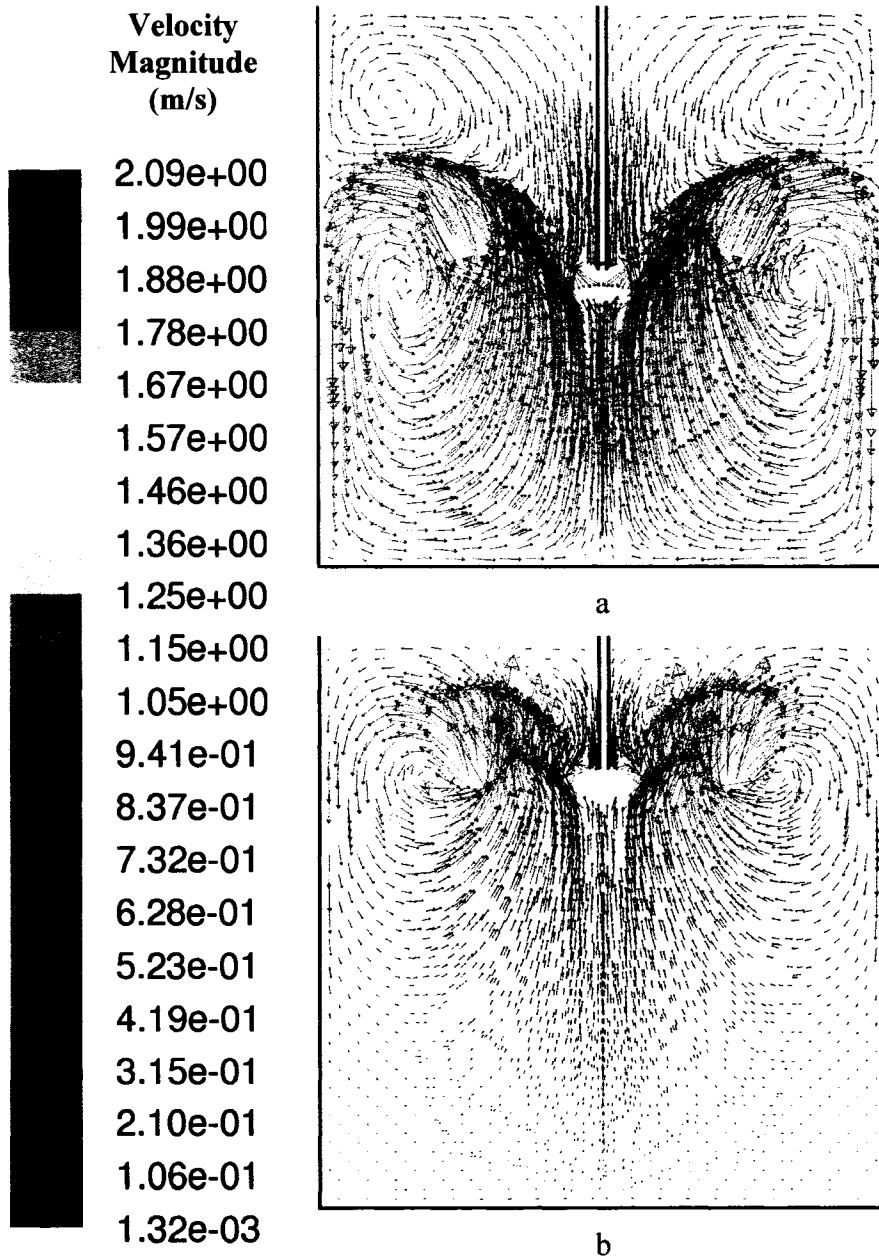
Figure 2.9: CFD simulation results for four full baffles with the PBTU. Velocity vectors in the mid-baffle plane at N_{jd} are shown for the following configurations: a. S = T/2, N_{jd} = 400rpm. b. S = T/4, N_{jd} = 230rpm.

Figure 2.11 shows the effect of submergence on cloud depth for the PBTU. Complete dispersion of particles into the liquid phase is easily achieved when the four baffle and one baffle configurations are used, but the cloud depth is again very small for the unbaffled case. These results are very similar to those obtained for the PBTD.

24
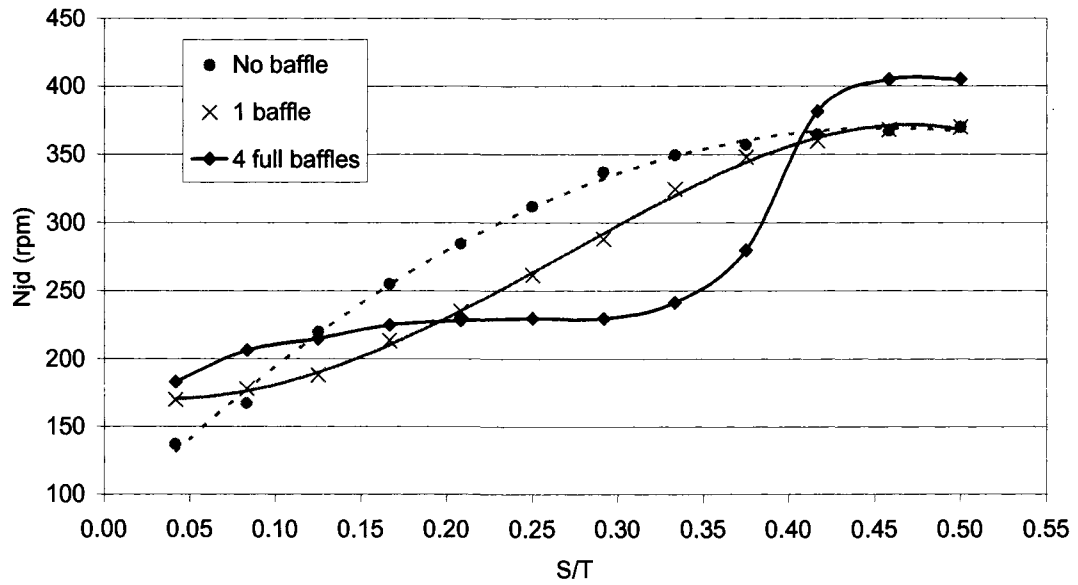
Figure 2.10: Effect of baffle configuration on N_{jd} for the PBTU ($D = T/2$, 2%v/v). The formation of a secondary loop close to the surface is the main reason for the sudden increase in N_{jd} at S/T $\cong$ 0.35 in the four full baffles configuration.
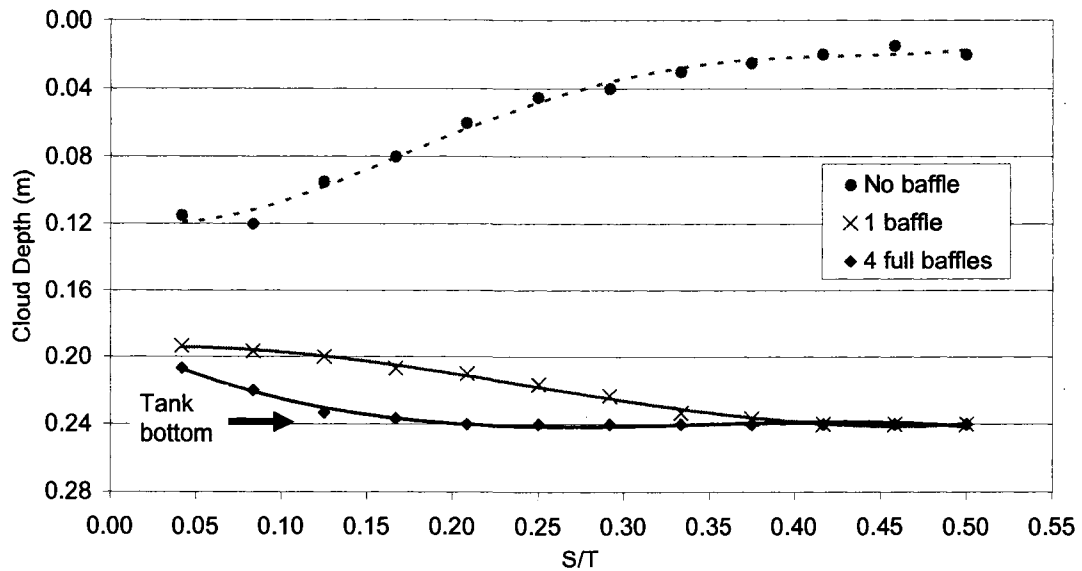
Figure 2.11: Cloud depth for the PBTU ($D = T/2$, 2%v/v). The strong top to bottom circulation drags the particles all the way to the bottom of the tank in the fully baffled configuration.

25

Observations of the flow for the A340 showed that the diameter and size of the surface vortex for both the unbaffled and the one baffle configuration are smaller than the ones seen with the PBTD and the PBTU. The A340 is a purely up-pumping impeller, while the PBTU and PBTD are both mixed flow impellers. Because of this, the A340 creates fast top to bottom circulation loops which reach the surface even for large values of S/T. This discharge flow quickly returns the particles to the surface, limiting the cloud depth, as shown in Figure 2.13.

For this impeller, the one baffle configuration performs better in terms of cloud depth than the fully baffled case for S/T>0.3, but higher values of N_{jd} are also required under these conditions.
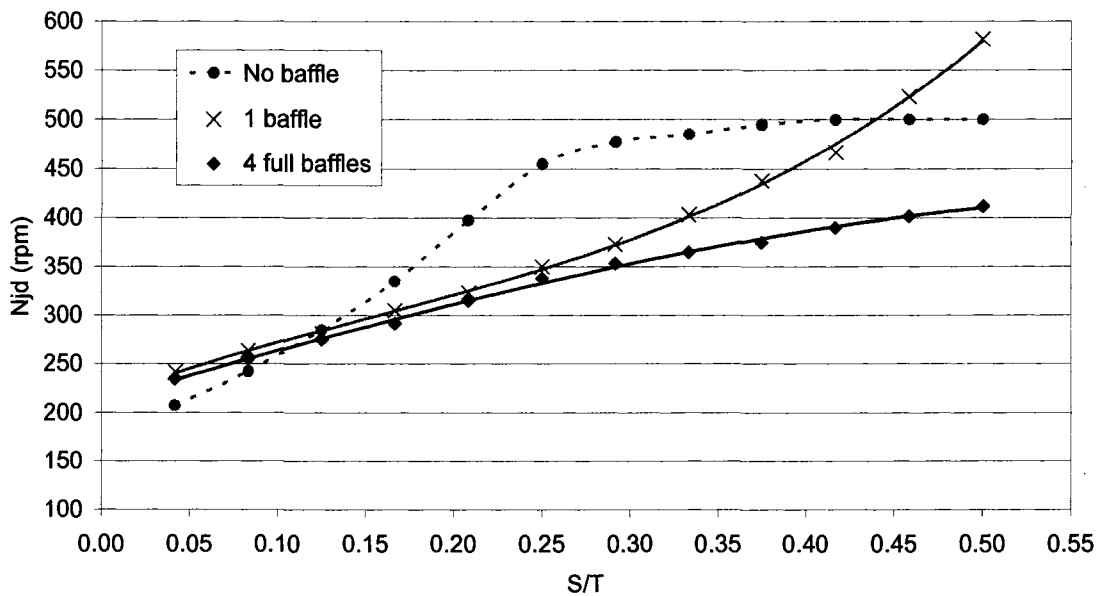
Figure 2.12: Effect of baffle configuration on N_{jd} for the A340 (D = 4T/9, 2%v/v). The discharge flow always reaches the surface due to the purely axial nature of the A340 impeller. Therefore, there is no sudden increase in N_{jd} for the fully baffled case in comparison with Figures 2.6 and 2.10.

26
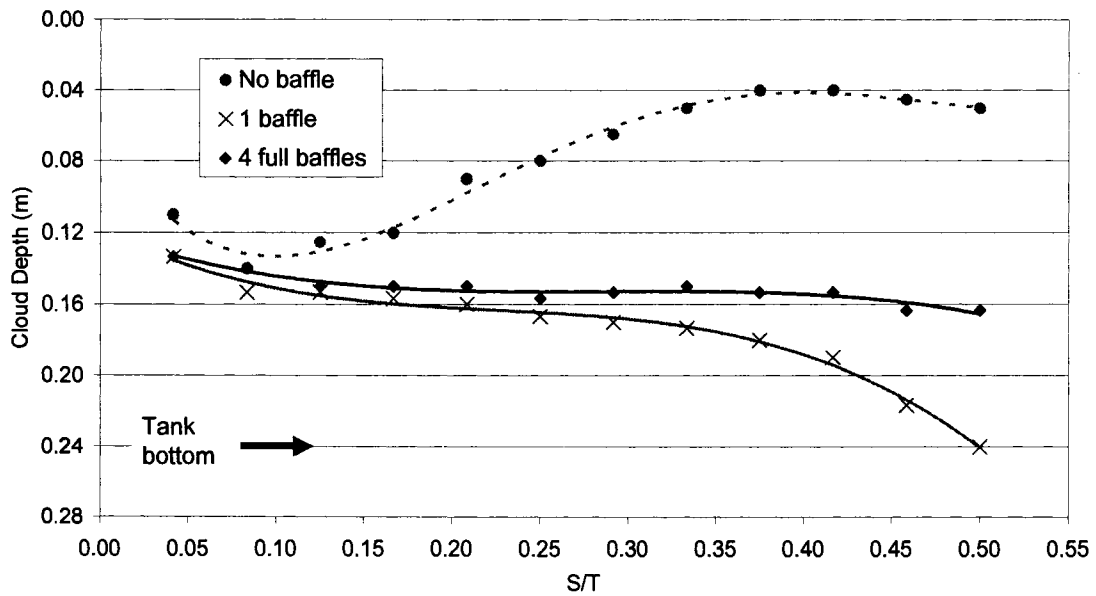
Figure 2.13: Cloud depth for the A340 (D = 4T/9, 2%v/v). The A340 is an up-pumping impeller which creates a very fast discharge flow directed toward the surface. This discharge flow rapidly returns the particles to the surface as soon as they are submerged and limits the maximum cloud depth.

A second set of experiments were run and are shown in Figure 2.14. These results show that an increase of the solids bulk concentration (%v/v) raises the values of N_{jd} obtained. From Figure 2.14a, it appears that the relationship between solids concentration and N_{jd} is linear. However, previous researchers found different results. Thring et al., (1990) concluded that an increase in concentration has a negligible effect on N_{jd} and suggested that N_{jd} is independent of concentration. Further experiments with a different solid/liquid pair confirmed that there is an influence of solids loading on the values of N_{jd} in Figure 2.14b. Again the trend is linear as Figure 2.14a. We conclude that there is an effect of concentration on N_{jd}, and that the relationship between solids concentration and N_{jd} is linear.

27
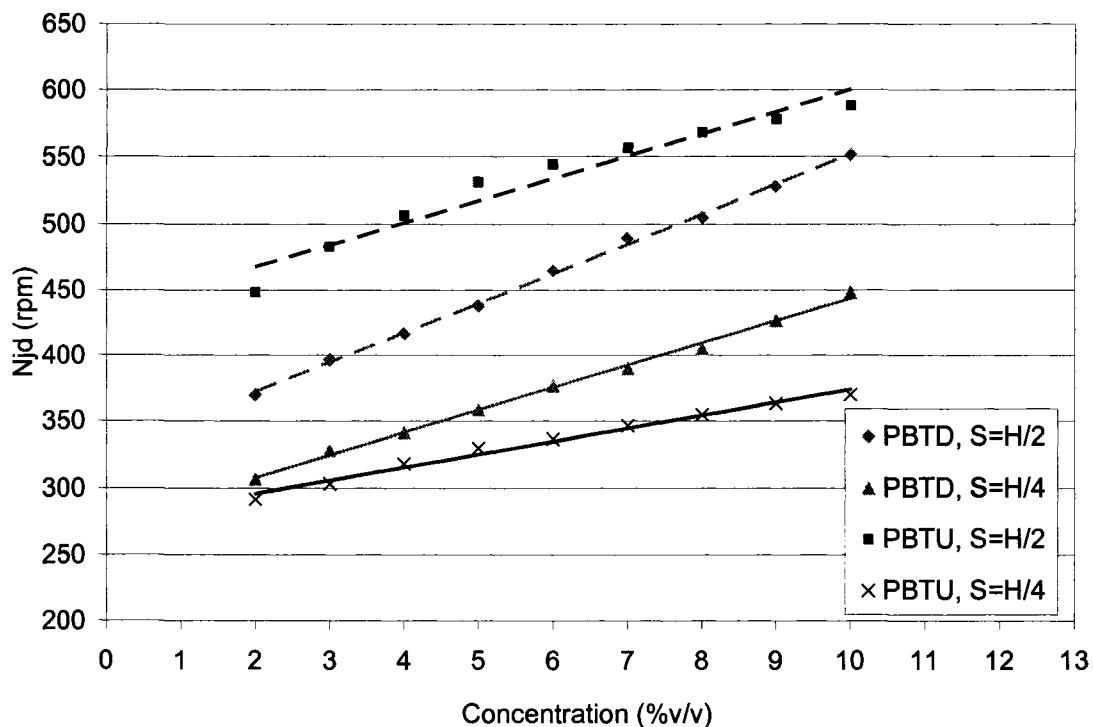
Figure 2.14a: Effect of submergence on Njd for the EPS beads 1 in water (PBTD and PBTU both with D = T/2, 4 full baffles). Note that the PBTU is particularly sensitive to submergence, performing much better than the PBTD for small submergences, but worse than the PBTD when the submergence is increased to T/2.

It is also apparent from Figure 2.14a and 2.14b that decreasing the impeller submergence results in a lower speed requirement for drawdown in both down- and up-pumping modes. When pumping up, the impeller discharge flow acts on the liquid surface to drawdown solids efficiently because of the turbulence and energy generated by the discharge flow, as described earlier. This is only observed when working at small submergences (S/H < 0.375).

At a larger submergences (S/H > 0.375) the performance of the up-pumping impeller decreases drastically in comparison with the down-pumping configuration. The energy that the PBTD uses in the recirculation loop to drawdown the solids is stable and strong over the range of submergences tested. The PBTU, on the other hand, depends on the impeller discharge flow for drawdown energy. When the submergence is small, the

28

discharge flow reaches the surface first, but as the submergence is increased to T/2, the discharge flow becomes completely submerged and reaches the wall before reaching the surface. At this point, a lot of the energy and mean flow are dissipated, or redirected downwards into the tank. This dramatically reduces the amount of energy available for solids drawdown. There are significant differences for the two pumping modes, and the PBTU performs much better at smaller submergences for the fully baffled configuration.
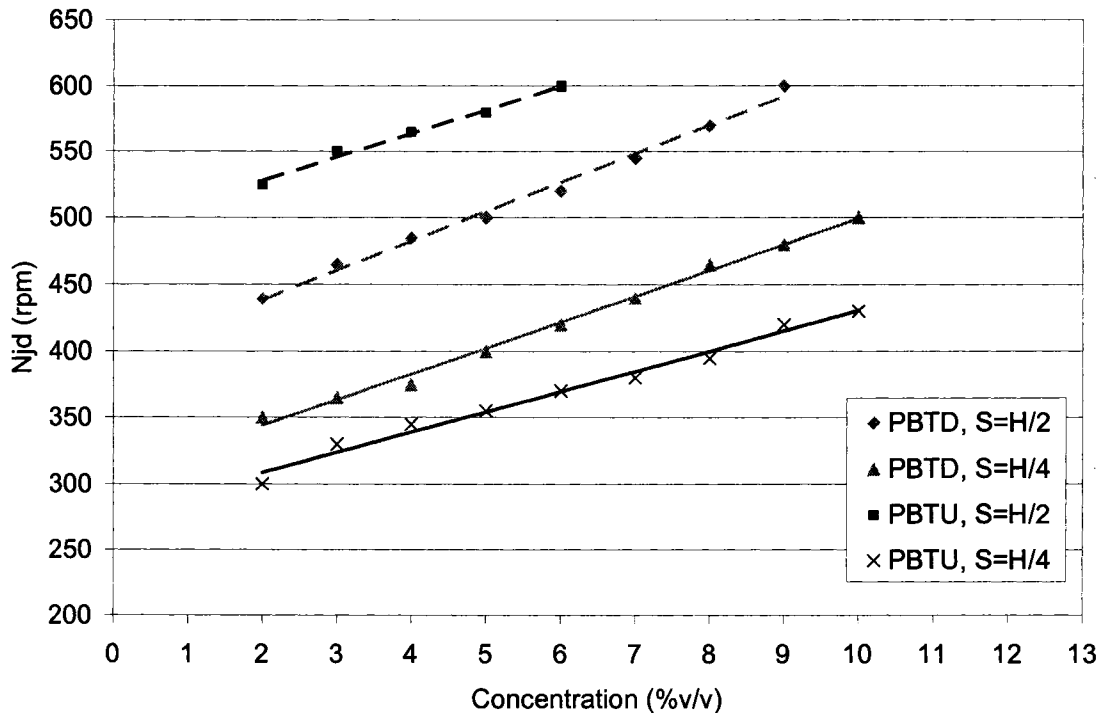
Figure 2.14b: Effect of submergence on Njd for the EPS beads 3 in Bayol (PBTD and PBTU both with D = T/2, 4 full baffles). Changing the wetting property of the solid has little impact in the results. The trend is the same as in Figure 2.14a.

To conclude the discussion of dominant mechanisms for solids drawdown, we turn to a quantitative analysis of the CFD simulations. Mean drag at the surface is clearly the main mechanism when the impeller is placed at large submergences, as shown in Figures 2.15a and 2.15b. The axial velocity at the surface (Figure 2.15a) is very large at large submergences, and very small at small submergences for both the PBTU and PBTD. An analysis of the turbulent kinetic energy values in Figure 2.15b complete the argument.

The turbulence is greater when the impeller is placed near the surface (S=T/4) and is much smaller for large S/T. This turbulence is observed in the experiments as waves, swirls or small vortex formations at the surface. The highest turbulent peak for the PBTD at S=T/4 confirms the presence of the fast eddies (turbulent fluctuations) around the shaft at the surface at small submergences, as observed in the experiments.
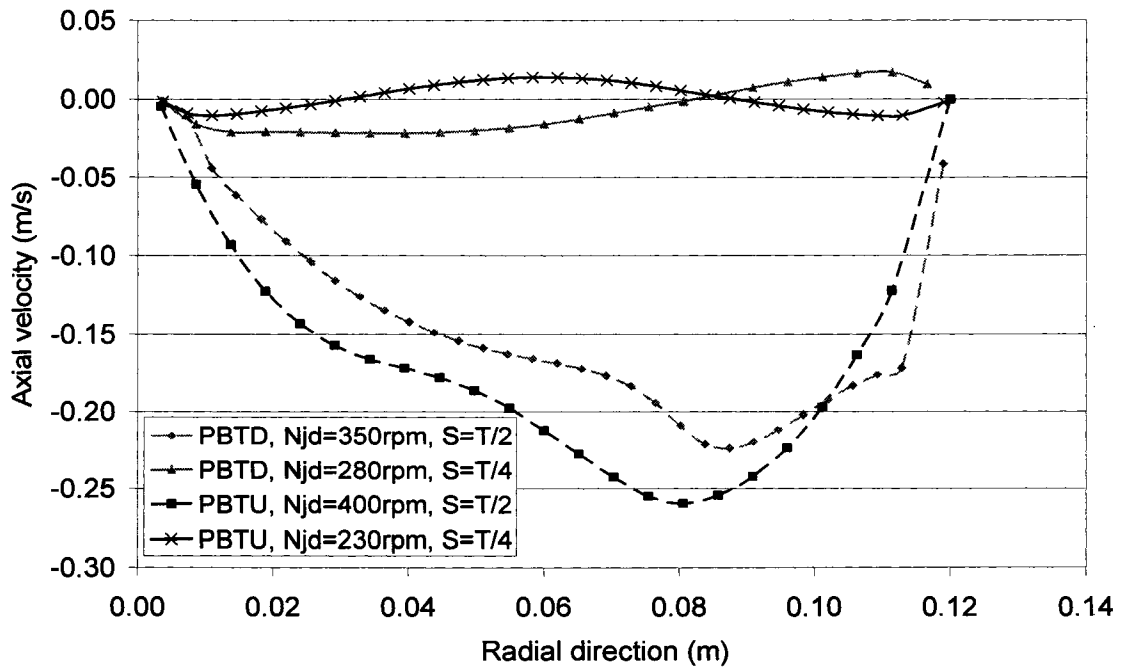
Figure 2.15a: Axial velocity at the surface calculated using CFD. The axial velocity is larger for S = T/2, indicating that mean drag is the main drawdown mechanism at large submergences.

30
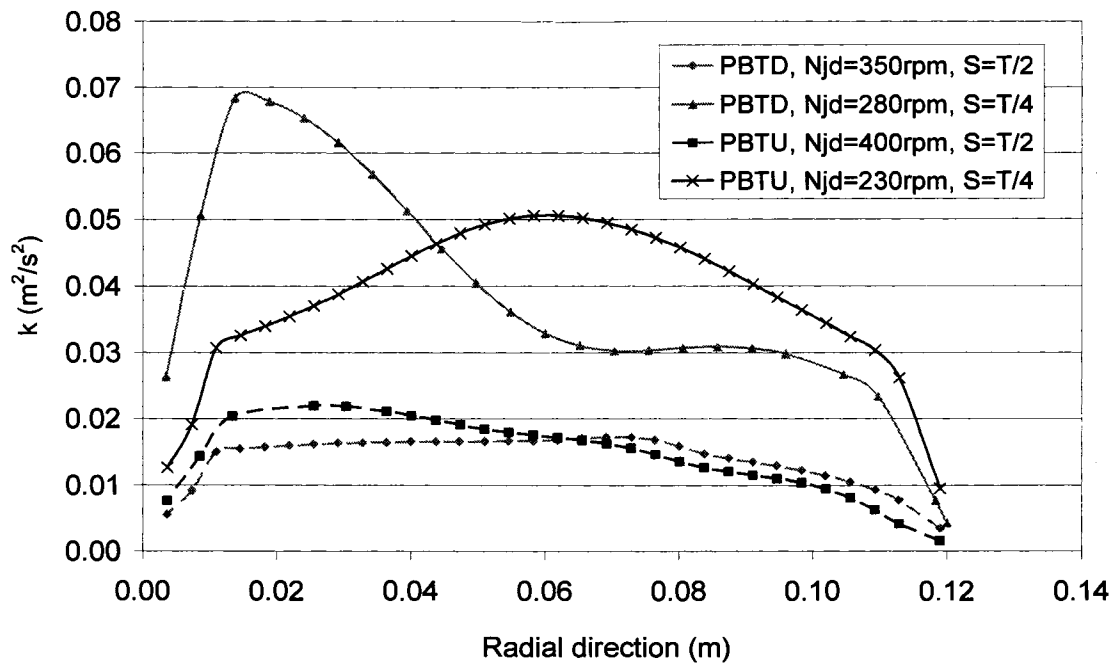
Figure 2.15b: Turbulent kinetic energy at the surface calculated using CFD. The k values are larger for S = T/4, indicating that turbulent fluctuations are the main drawdown mechanism at small submergences.

Finally, Figure 2.15c shows the radial velocity for the same four configurations. In this figure only the PBTU at S=T/4 has a positive (outward) radial velocity. Observations during the experiments agree with this behavior. This is the only simulated configuration where the solids are transported outward to the walls and then close to the wall a region of fast down flow draws the particles down into the tank. When the PBTU is used, the particles are drawn down in this region. For submergences close to T/2 and for all the submergences using the PBTD the opposite occurs. The particles in these configurations are driven towards the center and drawn down there.

31
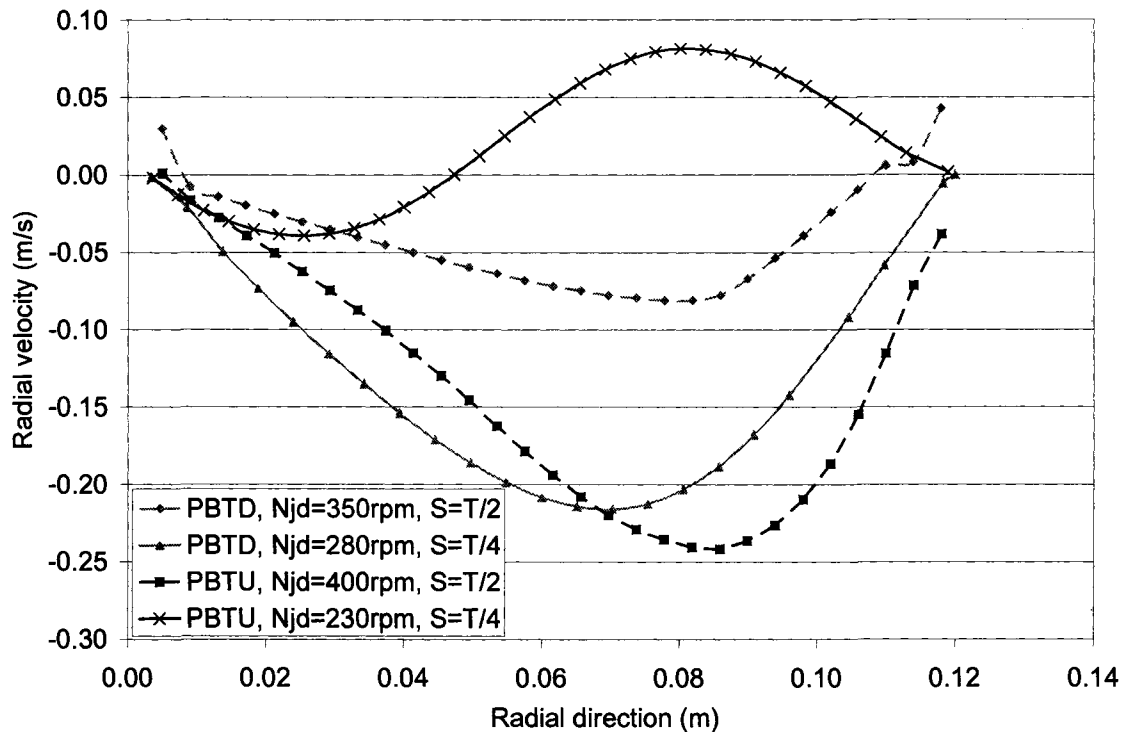
Figure 2.15c: Radial velocity profiles at the surface calculated using CFD at N_jd. For the PBTD, the flow at the surface is always towards the center (negative V_r), regardless of S. The (PBTU, S = T/4) data shows outward flow (positive V_r), as expected, while for (PBTU, S = T/2) the radial flow is towards the center due to the secondary circulation loop.

The final set of observations concerns the effect of the density difference on solids drawdown, as shown in Figure 2.16. The primary effect of density difference on N_{jd} from previous works (Joosten et al., 1977; Takahashi et al., 1999; Kuzmanic et al., 2001) is reflected by the exponent in the correlation by Joosten et al., (1977). In our experiments, the change in N_{jd} is also affected by the difference in density between the two phases, as shown in Figure 2.16. The explanation for this behavior is that an increase in $\Delta\rho$ means an increase of the buoyancy force, therefore additional mean velocity is needed to increase turbulent and drag forces in the vicinity of the surface to drawdown the particles. In the specific case when Bayol was used as the working fluid, the formation of a layer of foam retains the particles at the surface. This layer of foam is the reason why the values of N_{jd} obtained for the EPS beads 3/ Bayol system are significantly bigger even though the density difference is barely larger than with the EPS beads 2/ Water system.
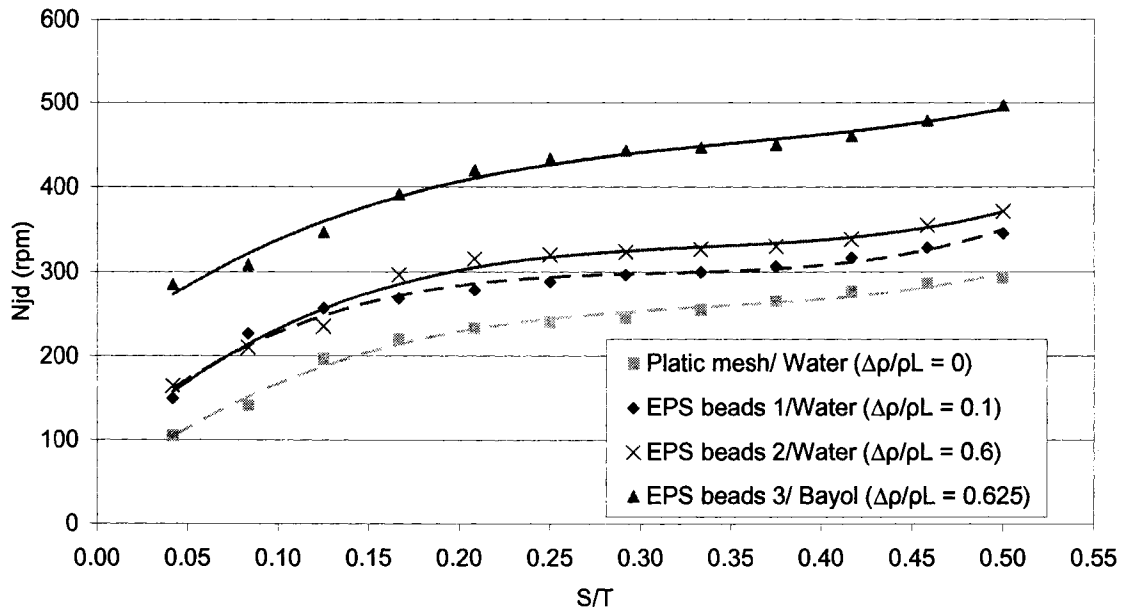
Figure 2.16: Effect of density difference between phases on N_{jd} with a solids concentration of 2%v/v for each solid-liquid system (PBTD D = T/2, 4 full baffles). Note that an increase in the density difference means an increase of the buoyancy force, therefore additional mean velocity (increased N) is needed to drawdown the particles.

2.5 Conclusions

Based on the experimental observations three mechanisms of drawdown of floating solids have been identified: deep vortex formation, mean drag and turbulent fluctuations. Deep vortex formation is less effective than turbulence and mean drag for solids distribution. The particles tend to collect on the surface of the vortex due to centrifugal separation. Turbulence, on the other hand, is the main mechanism at small submergences for both the PBTD and PBTU. The turbulent kinetic energy profiles from CFD simulations confirm this conclusion. Profiles of axial velocity at the surface show that mean drag is the main mechanism of solids drawdown for large submergences for both the down- and up-pumping impellers. Visual observations of the surface also support this conclusion. When comparing the three impellers in terms of the surface vortex, the A340 surface vortex is smaller in diameter and depth than the ones created by the PBTD and PBTU for both the unbaffled and the one baffle configurations.

33

Drawdown performance is sensitive to submergence for both PBT impellers, but much more so for the PBTU. This is due to the formation of a secondary circulation loop in the flow field. Visual observations suggest that the transition occurs close to S = 0.375. CFD simulations with a PBTU confirm this circulation pattern for the fully baffled configuration at S = 0.5. Experimental observations and the values of radial velocity at the surface show that the particles are drawdown in the vicinity of the shaft for all configurations. However the opposite occurs for smaller submergences (S < 0.375) with a PBTU impeller where the particles are drawn down close to the walls.

Using baffles to suppress surface vortex formation and increase mean velocity and turbulence at the surface is the best way to drawdown floating solids. The poor performance of the one-baffle and especially the unbaffled configuration in contrast with the fully baffled geometry support this conclusion. The four full baffles and a PBTD is the mixing geometry recommended among the conventional baffle configurations for large submergences, while for smaller submergences the results suggest the use of the up-pumping PBT instead.

Solids properties also affect N_{jd}, particularly the density and concentration. The relationship between solids concentration and N_{jd} is linear. This is contrary to the results reported by Thring et al., (1990). Finally, as the difference in density between the phases increase the velocity needed to pull the particles down (N_{jd}) increases as was expected.

34

Chapter 3

Novel Baffle Geometry

3.1 Introduction

The need to improve the performance of the mixing apparatus for drawdown of floating solids and the understanding gained from the experiments run with conventional baffle configurations led to a search for a better configuration. As concluded in Chapter 2, baffling suppresses the surface vortex formation and increases the intensity of mean drag and turbulence at the surface. Experimental observations and CFD simulations of the fully baffled configuration showed that strong top to bottom liquid circulation brings the particles rapidly back to the surface. Hence the next question arises "How deep should the baffles penetrate into the tank?" In the present chapter, two possible solutions to the problem are evaluated: the four half-baffles at the top, and the four surface baffles of height of 0.2T.

As in Chapter 2, the PBTD, the PBTU and the A340 are used to evaluate the effect of impeller type in the two new baffle configurations. CFD simulations were carried out for the surface baffles with the objective of explaining the experimental observations and supporting conclusions for the new configuration. Since power consumption is a key parameter for mixing processes, as well as N_{jd} an analysis of the power consumption at N_{jd} is completed for two different impellers and two different impeller diameters is reported. Measurements of the power number for the fully baffled and the surface baffled configurations are also reported.

35

3.2 Experimental

The same experimental methods described in Chapter 2 were used to explore the performance of the partial baffles. For these set of experiments Expandable polystyrene particles (EPS 1, SG = 0.9 and d_p = 1mm and EPS 3, SG = 0.3 and d_p = 2mm) were used in the experiments. Various baffle configurations were used: four full baffles (shown in Figure 2.1), four half-baffles at the top and four surface baffles (shown in Figures 3.1a and 3.1b respectively). All of the baffles had the same width (B_w = T/10) and baffle thickness (B_T = T/120).
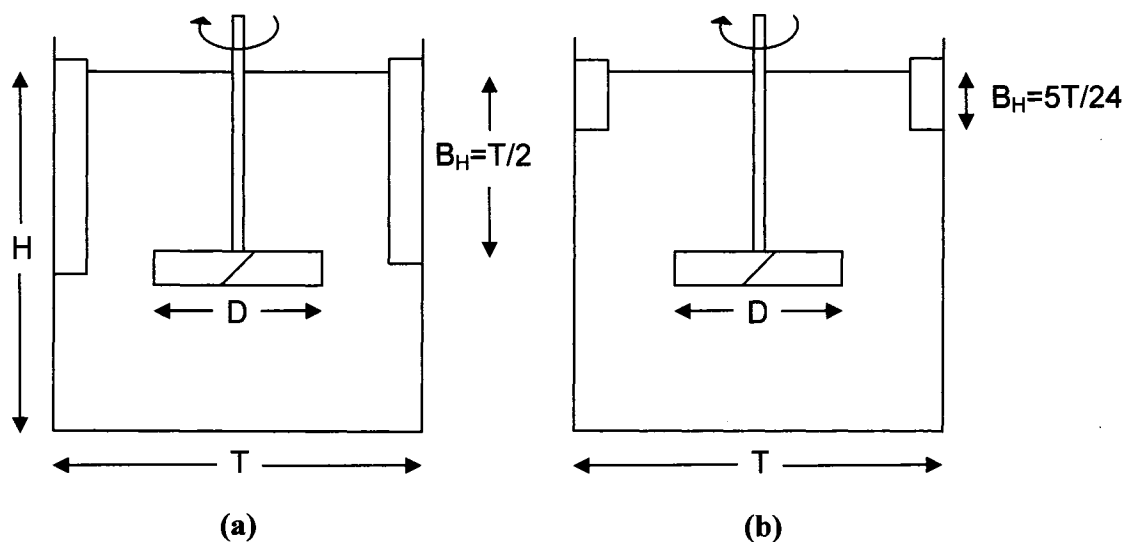
Figure 3.1: Schematic diagram of the half-baffle and surface baffle configurations studied.

The cloud depth, which is the perpendicular distance from the surface of the liquid to the point where the concentration of particles drops dramatically, was also measured for each configuration as is illustrated in Figure 3.2.
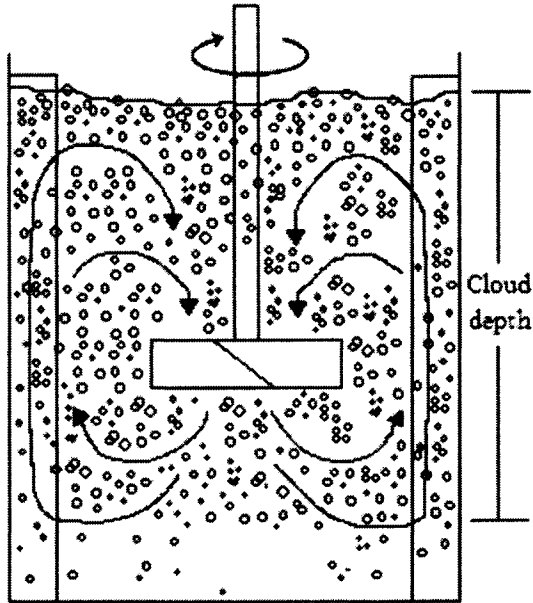
Figure 3.2: Illustration of cloud depth.

3.3 CFD protocol

The same CFD protocol described in Chapter 2 was used to explore the performance of the surface baffle configuration. Table 3.1 shows the different geometries simulated.

Table 3.1: Different geometries simulated

Configuration	1	2	3	4
Impeller type	PBTD	PBTD	PBTU	PBTU
Impeller diameter	D = T/2	D = T/2	D = T/2	D = T/2
Submergence	T/2	T/4	T/2	T/4
N_{jd}(rpm)	250	250	250	230

37

3.4 Results and discussion

Finding a new mixing configuration to improve the drawdown and subsurface retention of floating solids was our main objective. Two new baffle configurations were tested: four half-baffles situated at the top of the tank and four surface baffles that penetrated only through the upper radial recirculation part of the circulation loop to a depth of 0.2T. The aim of baffling only the surface is to suppress the formation of a big stable vortex which is not efficient for solids drawdown as shown in Chapter 2. Observations confirm that this objective is achieved and in most cases there is an improvement in the performance of the system in comparison with the fully baffled configuration. However; there are also significant differences in the performance when the two new configurations are compared. These results are presented in three parts. First, the performance of each of the three impellers is presented in terms of N_{jd} and cloud depth for each of the baffle configuration. These results are discussed in terms of the dominant mechanisms and the mean circulation patterns obtained from CFD simulations. Second, the PBTU impeller is used to examine the effect of different baffle configurations on the power number (Np). The up and down-pumping PBT impellers are compared with each other to see the influence of impeller diameter and pumping mode on the results of N_{jd} and power consumption. Finally, two different specific gravities for the EPS and two types of liquids are used to analyze the effect of fluid and solids properties on the values of N_{jd}.

3.4.1 PBTD impeller

The PBTD impeller is the most widely used mixed flow impeller. Many investigators (Özcan-Taskin et al., 2001; Takahashi et al., 1999; Thring, 1990; Joosten et al., 1977) report that mixed flow impellers perform better than radial or purely axial impellers for solids drawdown. Here, the PBTD is studied in terms of N_{jd} and cloud depth for three different baffle configurations. The flow patterns generated by this impeller using the surface baffles configuration are presented. These flow patterns were obtained from CFD simulations and are used as a base for interpretation and discussion of the results.

38

Figure 3.3 shows the flow field at N_{jd} for the surface baffles configuration at two submergences of the PBTD. From these results we can see the direction, magnitude of flow, and the size of the recirculation loops present. The small dots observed under the main axial circulation for both submergences (Figures 3.3a and 3.3b) show velocity vectors coming in and out of the plane. These vectors clearly indicate that below the impeller this configuration creates mainly tangential flow. With surface baffles, the mean circulation drags the particles from the surface and then the tangential flow distributes them throughout the tank. This was also observed in the experiments.

Observations during the experiments show that the half-baffle configuration does not significantly change the drawdown, distribution of particles and retention time performance. The behavior of this configuration is comparable to the fully baffled case and the values of N_{jd} confirm the visual observations. Four half-baffles are enough to create the full top to bottom circulation loops that pull down the particles similar to the four full baffles configuration. The major difference observed when comparing both configurations is that a few particles spin in a tangential flow at the bottom of the tank when the half-baffles are used, while for the four full baffles the particles stay in the main circulation loop.
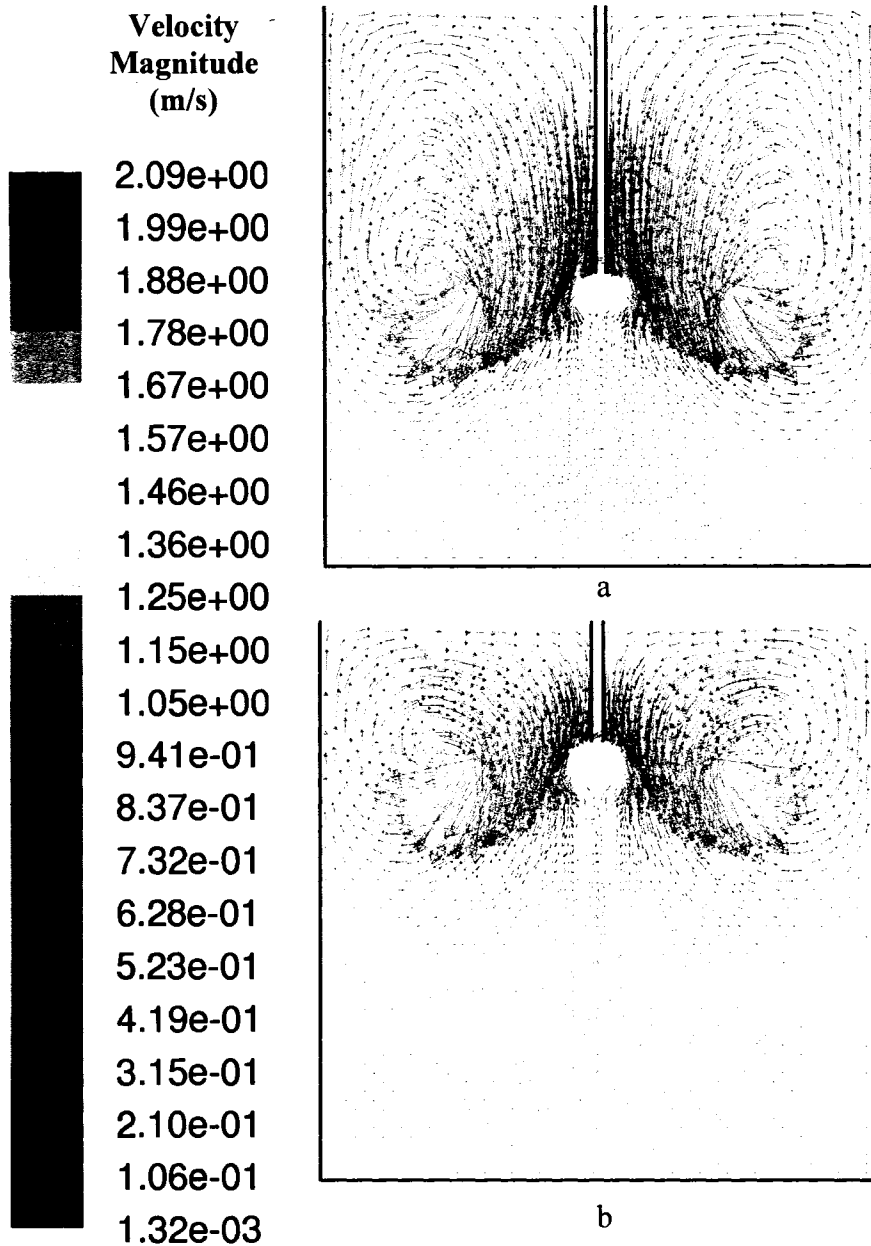
Figure 3.3: CFD simulation results for the four surface baffles with the PBTD. Velocity vectors in the mid-baffle plane at N_{jd} are shown for the following configurations: a. $S = T/2$, $N_{jd} = 250$rpm. b. $S = T/4$, $N_{jd} = 250$rpm.

While running the experiments with the surface baffles it was clear that mean drag and turbulent fluctuations are responsible for the drawdown of particles. The presence of baffles at the surface suppresses the single big vortex formation. Instead, a small vortex instantly appears in the vicinity of the shaft at the surface. This is the main zone where the particles are drawn down. Once the particles are below the baffles, they swirl down in

40

the vortex toward the bottom of the tank. This behavior can be explained in the context of the circulation created. A predominant tangential velocity component is present in the bottom of the tank, as seen in Figure 3.3. This circulation is created because of the lack of baffles in this zone. The tangential circulation gives a better distribution and seems to provide larger values of residence time of fully submerged particles in the tank. It can be seen in Figure 3.4 that with the use of the surface baffles we are able to reduce the values of N_{jd} at large S/T. It seems that by cutting off the bottom of the baffles, the drag in the middle and bottom zones of the tank is eliminated, forcing all of the dissipation and turbulence toward the surface. Even at big submergences, most of the energy dissipation is available for solids drawdown at the surface.
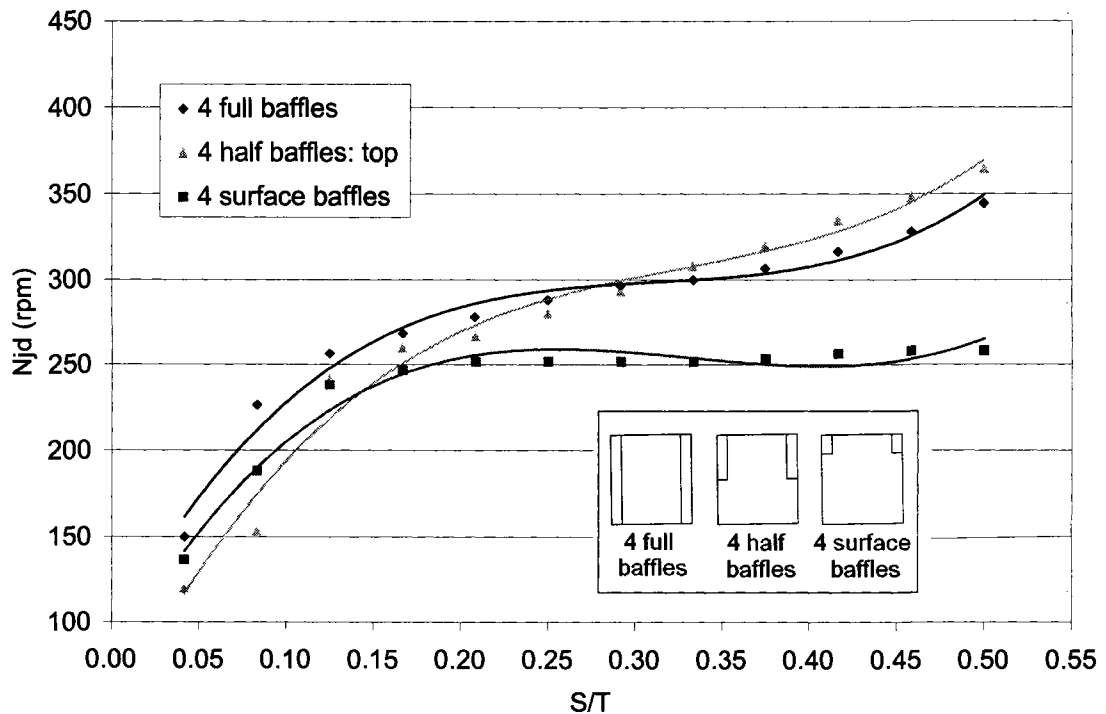
Figure 3.4: Effect of baffle configuration on N_{jd} for the PBTD (D = T/2, 2%v/v). Note that there is no significant difference between the fully baffled and the four half-baffle configurations. Instead, the 4 surface baffles configuration performs better than the other two baffle configurations (major reduction in the Njd values).

Cloud depth is another way to quantify the distribution of the particles in the tank, but can not be assumed to be proportional to the residence time of the particles below the surface. In Figure 3.5 for the down-pumping impeller, the values of cloud depth for both

41

the fully baffled and the surface baffles configurations are similar. However, the residence time for the surface baffle configuration seems to be higher than for the fully baffled configuration. No direct measurement was made during the experiments. The reason for this behavior is the tangential flow created in the bottom half of the tank by the surface baffles in comparison with the main circulation loop present with the four full baffles. The circulation loop brings the particles back to the surface almost immediately, while the tangential flow keeps them below the surface. Figure 3.5 also shows the poor performance of the four half-baffles in comparison with the other configurations studied. The reason for this behavior is the intensity of the main circulation. For the four half-baffles the circulation loop is weaker than for the four full baffles and so the cloud depth is much smaller, while with the surface baffles the circulation pattern and mechanism of solids distribution changes entirely. For the PBTD, the half-baffles are a poor choice, and the surface baffles offer the best drawdown performance at large submergences.

Figure 3.5: Cloud depth for the PBTD (D = T/2, 2%v/v). The distribution of particles is similar for the fully baffled and the surface baffles configurations; however, it is important to point out that the circulation time below the surface for the particles is longer with the surface baffles.
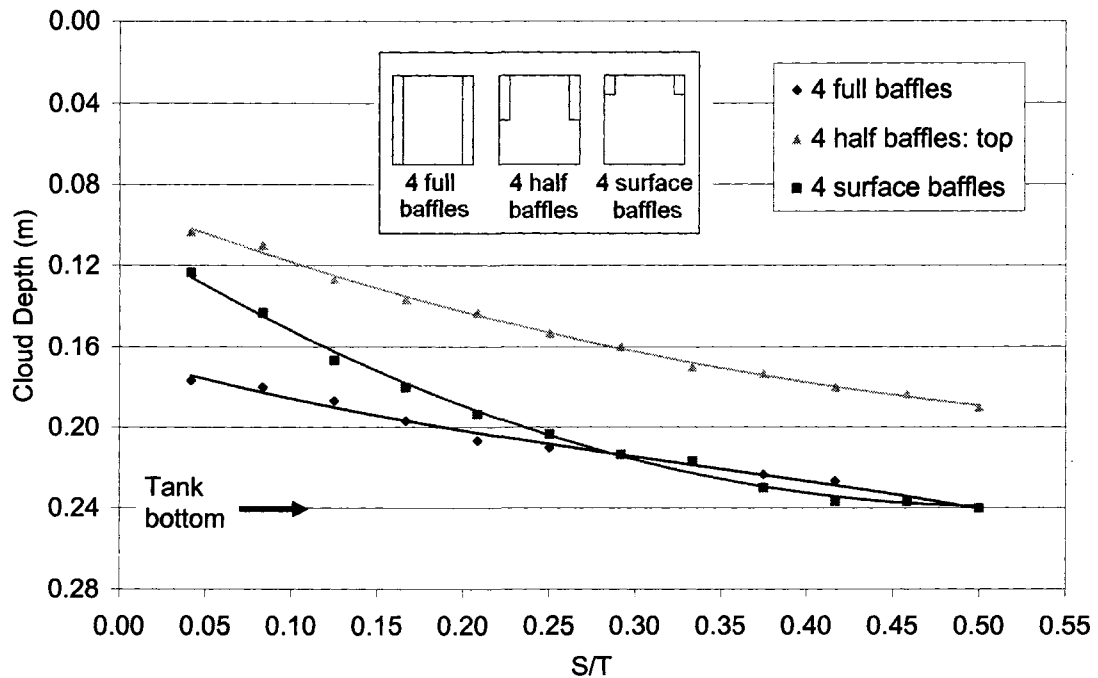
42

3.4.2 PBTU impeller

The up-pumping axial impellers were first employed in the early 1980's when it was discovered that the up-pumping configuration could be beneficial for efficient dispersion of gases in gas-liquid mixtures. In recent years, these impellers have found their use in several other areas of operation (Nienow and Bujalski, 2004), and their value is increasing substantially throughout the industry processes.

When the PBTU is used at large submergences with full height baffles, the discharge flow of the impeller hits the wall before it reaches the surface and a secondary loop is formed (Chapter 2). The velocity vectors at the surface for this secondary loop are very small (Figure 2.9). When surface baffles are used with large submergences, the secondary circulation loop still forms, but most of the flow and turbulence is now concentrated at the surface, as shown in Figure 3.6a. With surface baffles, the discharge flow of the PBTU impeller at S/T = 0.5 goes directly to the tank wall where it gets split into two circulation loops with roughly equal flow, one below and one above the impeller. This circulation pattern resembles a radial impeller more than a mixed flow impeller, and once again reveal the strong interactions between the PBT flow field and the tank geometry.

When a smaller submergence was simulated (Figure 3.6b), no significant differences were observed in comparison with the CFD simulations for the fully baffled case (Chapter 2). As with the full baffles, the discharge flow of the impeller reaches the surface quickly and most of the turbulent kinetic energy generated by the impeller is dissipated at the surface drawing down the particles.

43
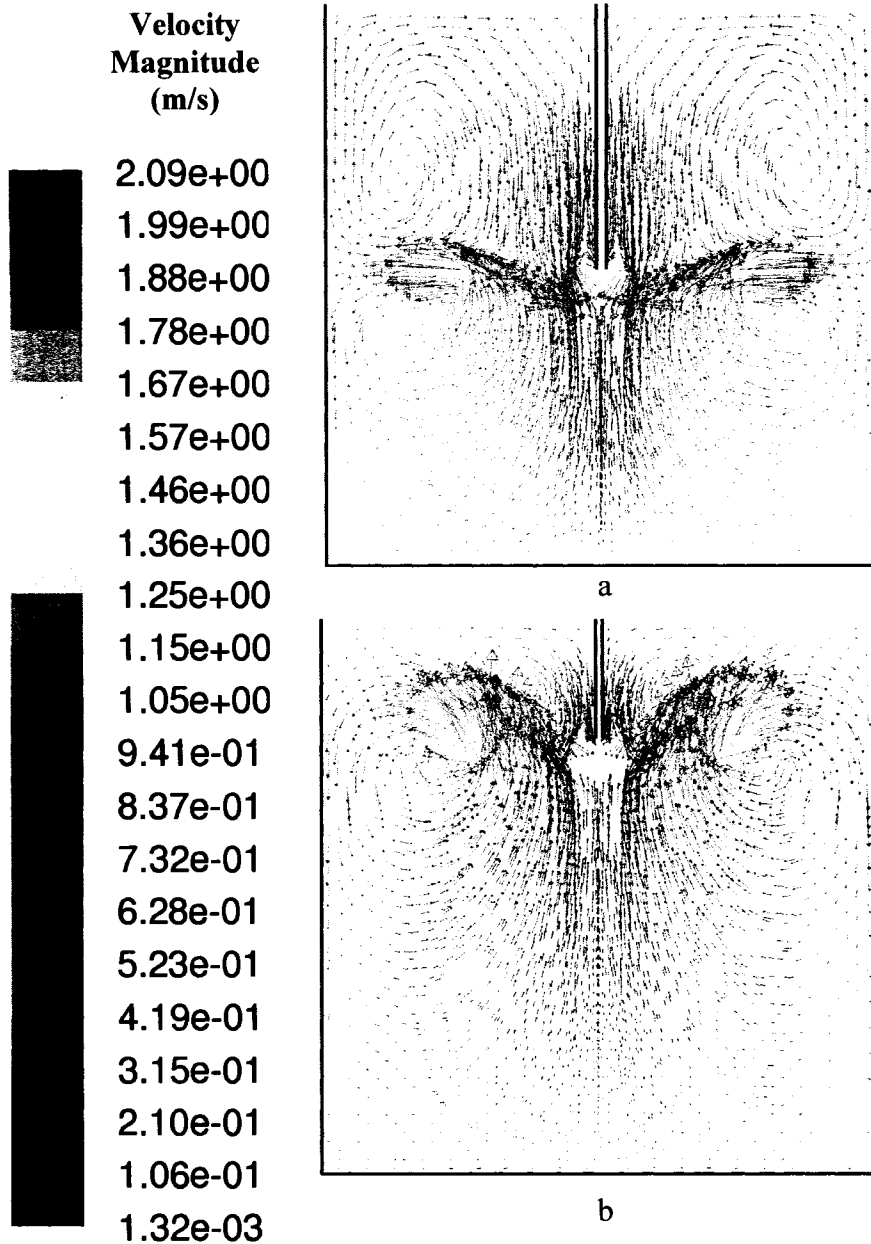
Figure 3.6: CFD simulation results for the four surface baffles with the PBTU. Velocity vectors in the mid-baffle plane at N_{jd} are shown for the following configurations: a. $S = T/2$, $N_{jd} = 250$rpm. b. $S = T/4$, $N_{jd} = 230$rpm.

Figure 3.7 shows the N_{jd} results for the PBTU for all three baffle configurations. For the surface baffles, N_{jd} becomes almost constant once S/T is higher than 0.25. This behavior allows us to place the impeller deeper in the tank without having to increase the speed to achieve drawdown of particles. One of the advantages of placing the impeller at a larger submergence is to avoid air entrainment. In most processes, as suggested by Özcan-

44

Taskin (2001), prevention of air or vapour entrainment from the headspace may be required to ensure the desired product quantity and quality. Another advantage is that placing the impeller at larger values of S results in larger values of cloud depth. Figure 3.7 shows that, as for the PBTD, the N_{jd} for four half-baffles matches the N_{jd} for the four full baffles. A secondary circulation loop is also observed with the half-baffles when the impeller is placed at S/T larger than 0.35, the same submergence where N_{jd} increases rapidly.
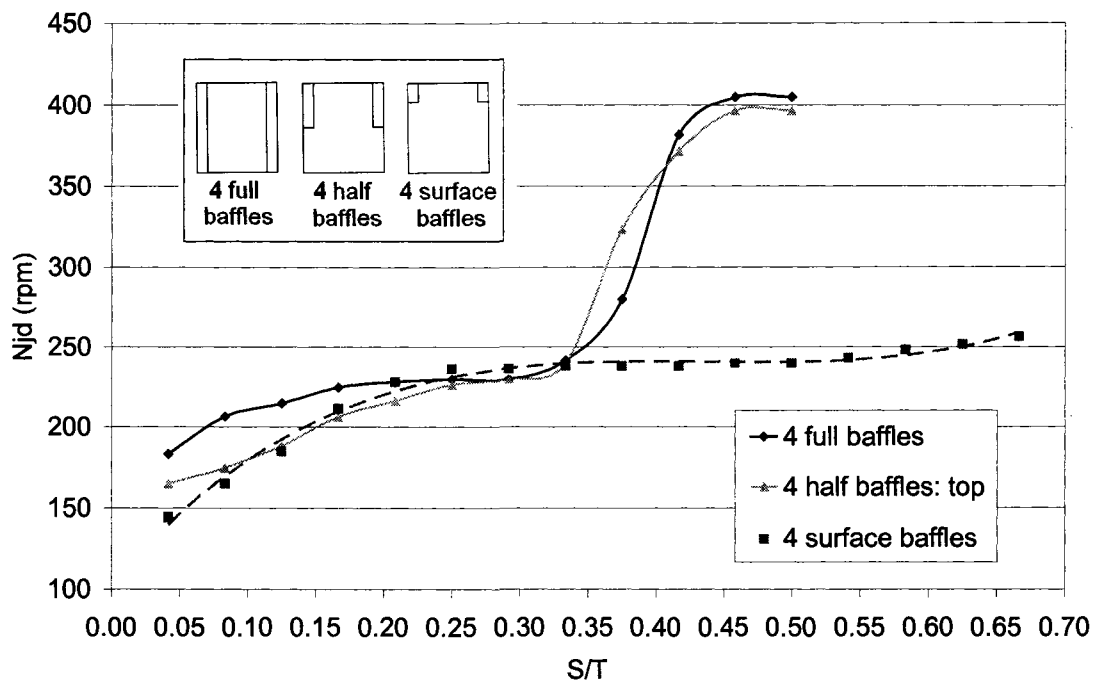
Figure 3.7: Effect of baffle configuration on N_{jd} for the PBTU (D = T/2, 2%v/v). The formation of a secondary circulation loop close to the surface is the main reason for the sudden increase in N_{jd} at S/T $\cong$ 0.35 for the half-baffles and the full baffles. In contrast, the flow pattern for the surface baffles promotes the drawdown of the particles even for large values of S.

Moving now to the cloud depth for the PBTU, shown in Figure 3.8, the cloud depth for the surface baffles configuration is initially lower than for the four full baffles. However; the ability to place the impeller at larger submergences without increasing N_{jd} allows the surface baffles to achieve complete dispersion of solids at a lower N_{jd} than the four full baffles configuration. During the experiments we observed that most of the ingested

45

particles remain close to the surface in the upper circulation loop for the fully baffled configuration. It is difficult to identify a sudden drop in concentration for this configuration in marked contrast with the other configurations studied. With the surface baffles the distribution is more uniform along the tank and the drop in concentration is clearer. Baffle height strongly influences the flow patterns in the tank and has a large impact on the distribution of solids.
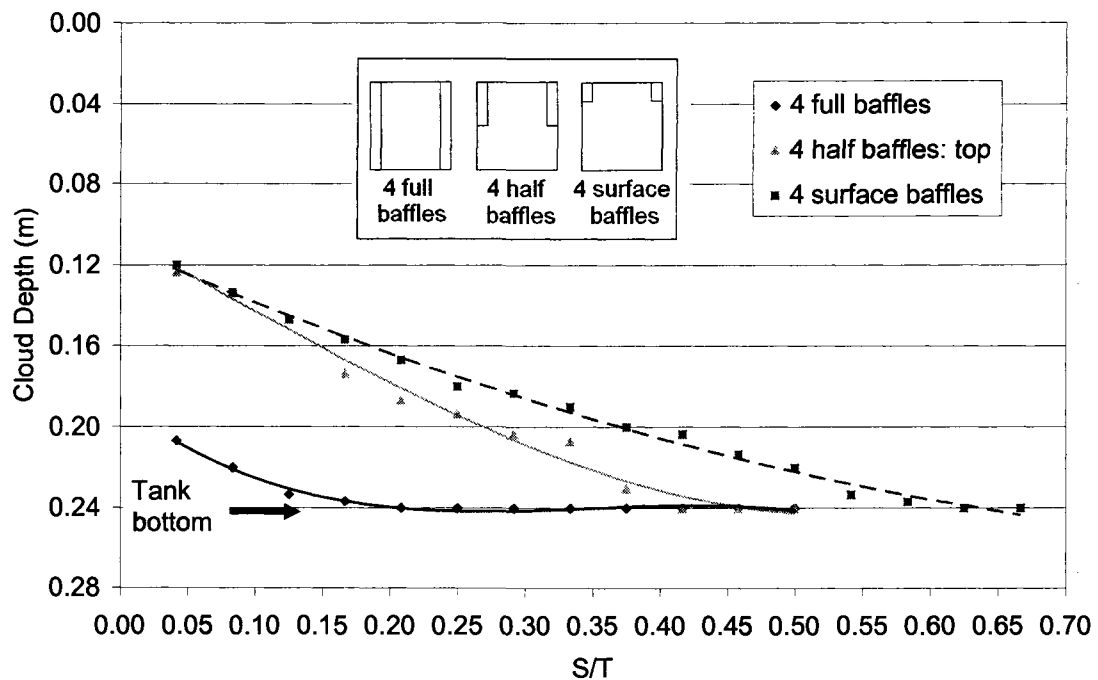
Figure 3.8: Cloud depth for the PBTU (D = T/2, 2%v/v). The ability to place the impeller at a submergence larger than T/2 allows the surface baffle configuration to achieve a good particle distribution. Note that the higher the submergence of the impeller, the smaller the risk of air entrainment in the system.

3.4.3 A340 impeller

The Lightnin A340 is the last impeller studied with partial height baffles. It is recommended for up-pumping applications (Gigas, 2005). The A340 is ideal for multi-phase processes, such as fermentation, polymerization and hydrogenation. For this impeller, the values of N_{jd} and cloud depth are given in Figures 3.9 and 3.10. It can be

46

seen that decreasing the impeller submergence results in lower speed requirement for drawdown (N_{jd}), similar to the other two other impeller configurations studied. However, when the A340 impeller is used, N_{jd} is higher than for the PBTU or the PBTD. Since the impeller diameter of the A340 is smaller, this is to be expected. The reader is also reminded that power draw of the A340 is less than that for the PBT at the same N and D.

When the A340 impeller is used, different baffle configurations do not affect the performance of the impeller, because even for large values of submergence the flow is steady and stable. What this means is that the impeller creates the same flow field within the tank for the different submergences studied, regardless of the baffle geometry. Experiments show that the discharge flow always reaches the surface when the A340 is used because of the axial nature of the impeller. There is no significant difference in the values of N_{jd} obtained for the different baffle configurations.
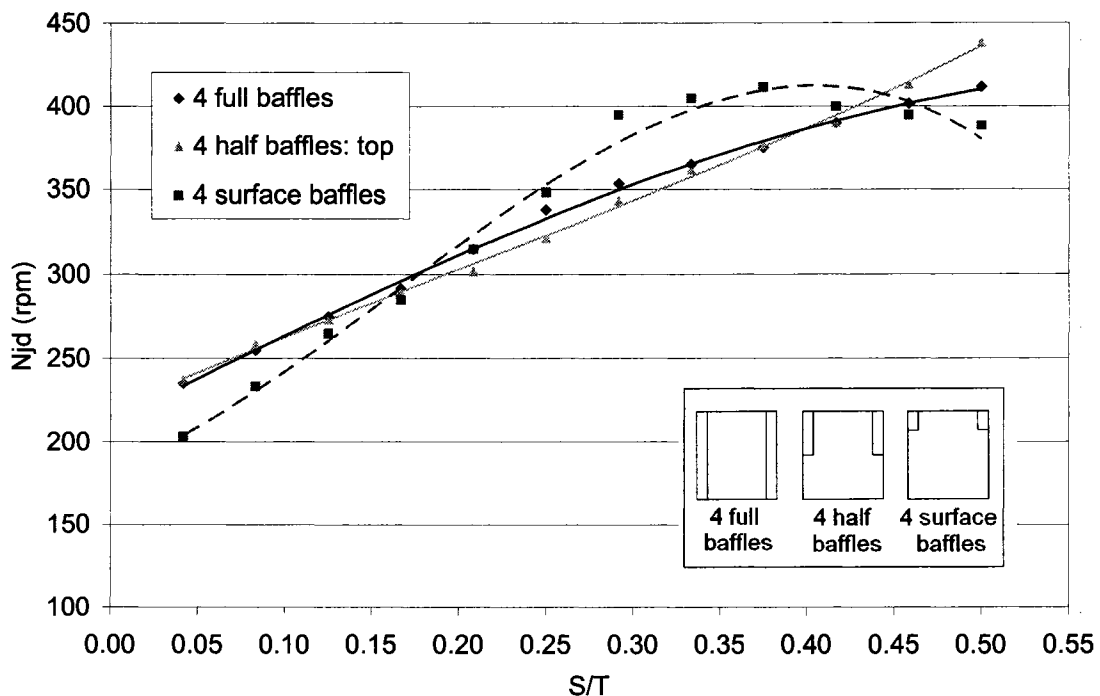
Figure 3.9: Effect of baffle configuration on N_{jd} for the A340 (D = 4T/9, 2%v/v). The discharge flow always reaches the surface due to the purely axial nature of the A340 impeller. For this impeller, there is no effect of the different baffle configurations on N_{jd}.

47

While the N_{jd} performance is very stable, the performance in terms of cloud depth and particle distribution obtained is significantly poorer for the A340 (Figure 3.10). For large submergences (S/T > 0.3) the cloud depth is approximately 33% smaller than for the PBT's. The reason is the high intensity of the circulation loop created by the impeller. The A340 creates a big suction zone below the impeller which does not allow the particles to go deep in the tank. This suction carries the particles back to the main circulation, from where they are pushed towards the surface.
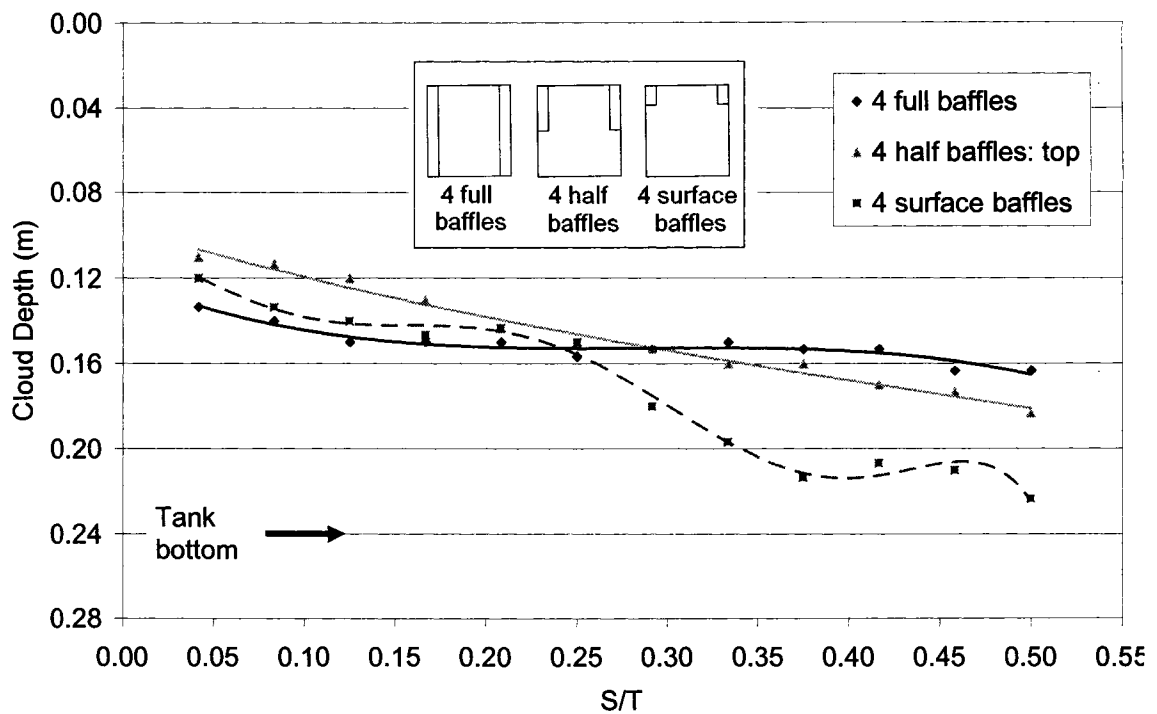
Figure 3.10: Cloud depth for the A340 (D = 4T/9, 2%v/v). The lack of baffles from S > T/5 for the surface baffles promotes a tangential flow that in combination with the axial flow created by the A340 impeller improves the particle distribution in comparison with full baffles and half-baffles.

3.4.4 Reducing the impeller diameter for the PBTU and PBTD

Figure 3.11 shows the effect of baffle configuration on N_{jd} for the T/3 PBT impeller in both down and up-pumping mode. For the small up-pumping impeller, the fully baffled

48

configuration performs better than the surface baffle configuration. The reason for this behavior, as observed and described by Özcan-Taskin and Wei (2003), is that the discharge flow of the T/3 PBTU impeller is strongly axial. Hence, the discharge of the impeller is in the direction of the surface even for large submergences. While for the T/2 PBTU impeller the strong radial component of the impeller discharge reaches the tank wall and forms a secondary circulation loop, the small PBTU does not. The small down-pumping PBT gives poor performance for both the fully baffled and surface baffle case. The small impeller in the down-pumping mode creates less circulation and less mean drag, which is the main drawdown mechanism for this configuration. It is important to note that for the T/3 PBTD using the fully baffled configuration was impossible to obtain values of N_{jd} for S/T > 0.25. Larger impeller diameters perform better for drawdown of floating solids.
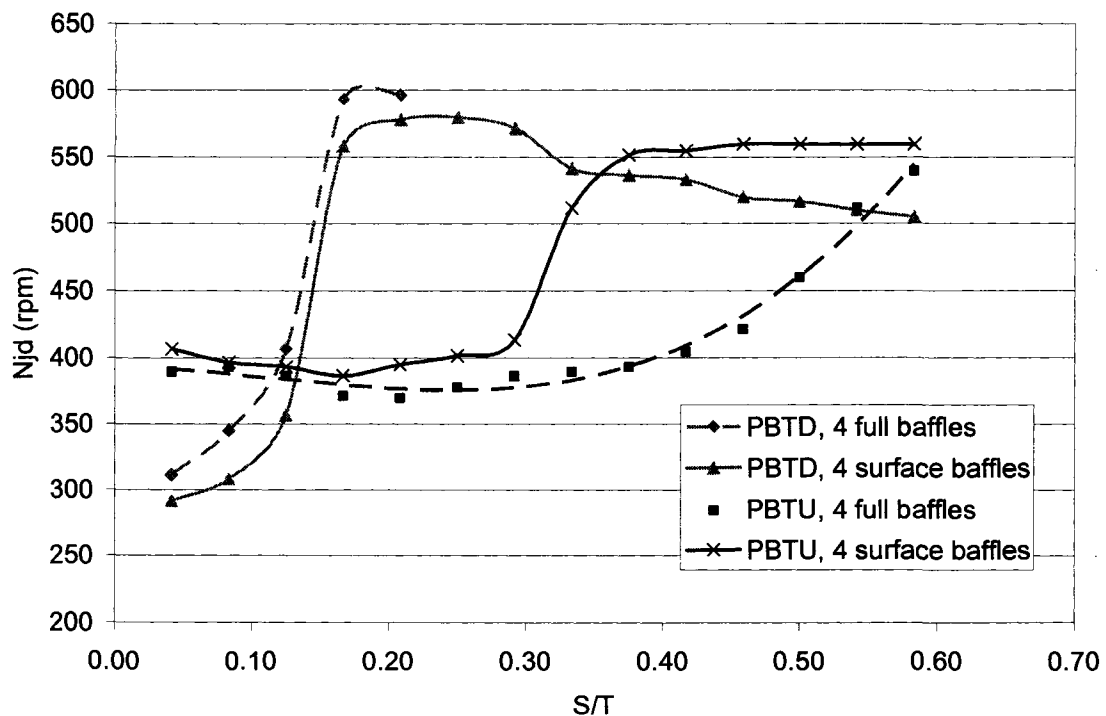
Figure 3.11: Effect of baffle configuration on N_{jd} for the PBTD and PBTU (D = T/3, 2%v/v). Note that the strong axial component of the impeller discharge is the main reason for the good performance of the smaller PBTU impeller.

49

3.4.5 Power consumption

A set of experiments were run to determine Np for the fully baffled and surface baffles configurations. The methodology used to obtain the power number for the different configurations is described in the paper by Chapple and Kresta (2002). Figure 3.12 shows Np in terms of Reynolds number for both baffle configurations at two different submergences. We observe that there is a small effect or no effect of submergence in the value of Np. The influence of submergence is apparent instead as the point of air entrainment. Surface aeration is responsible for the sudden decrease in Np in all the curves in Figure 3.12 at high values of Reynolds number. Bubbles of air enter into the liquid bulk from the head space and then progressively reach the impeller region. The slight influence of submergence on the values of Np is because there are no significant changes in the flow pattern from one submergence to the other. Finally, Figure 3.12 shows that the average value of Np is not significantly different for the two baffle configurations studied.
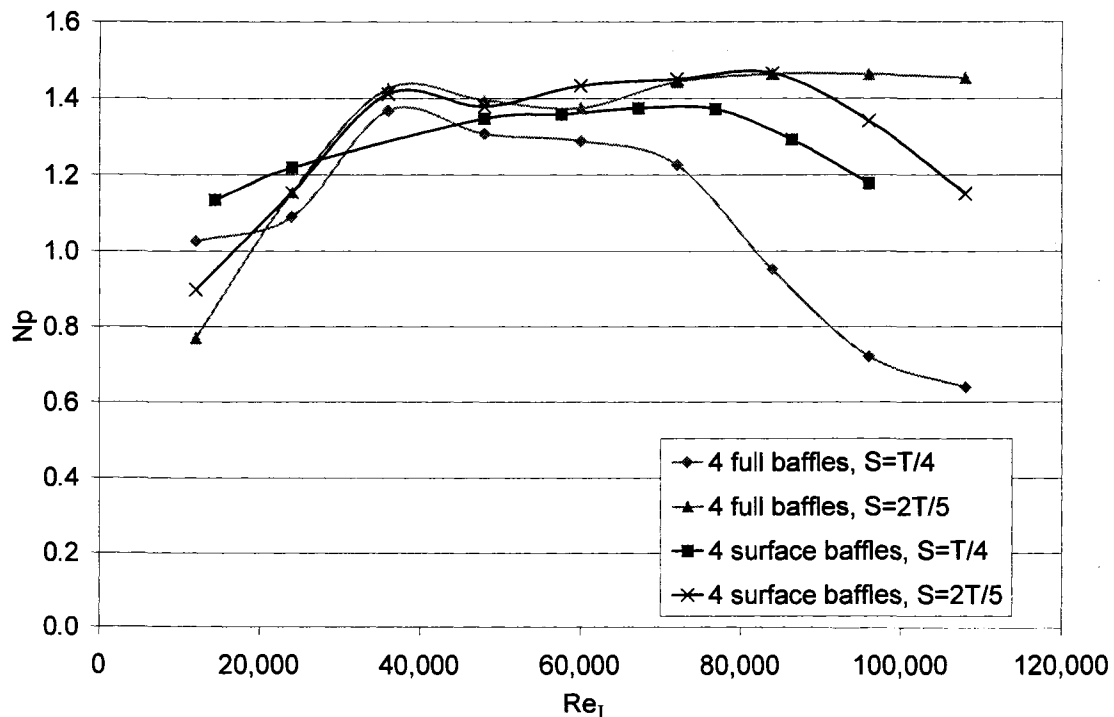
Figure 3.12: Effect of baffle configuration on Np for the PBTU (D = T/2, 2%v/v). The onset of surface aeration is responsible for the sudden drop at large values of Reynolds number.

50

For the smaller impeller (D=T/3), the results obtained (Figure 3.13) also show that there is no significant difference in the values of Np for full or surface baffles. These values are 1.27 for the four full baffles configuration and 1.24 for the surface baffles configuration. The sudden drop around Re=20,000 is attributed to the change of flow regime from transitional to turbulent flow type for the smaller impeller.
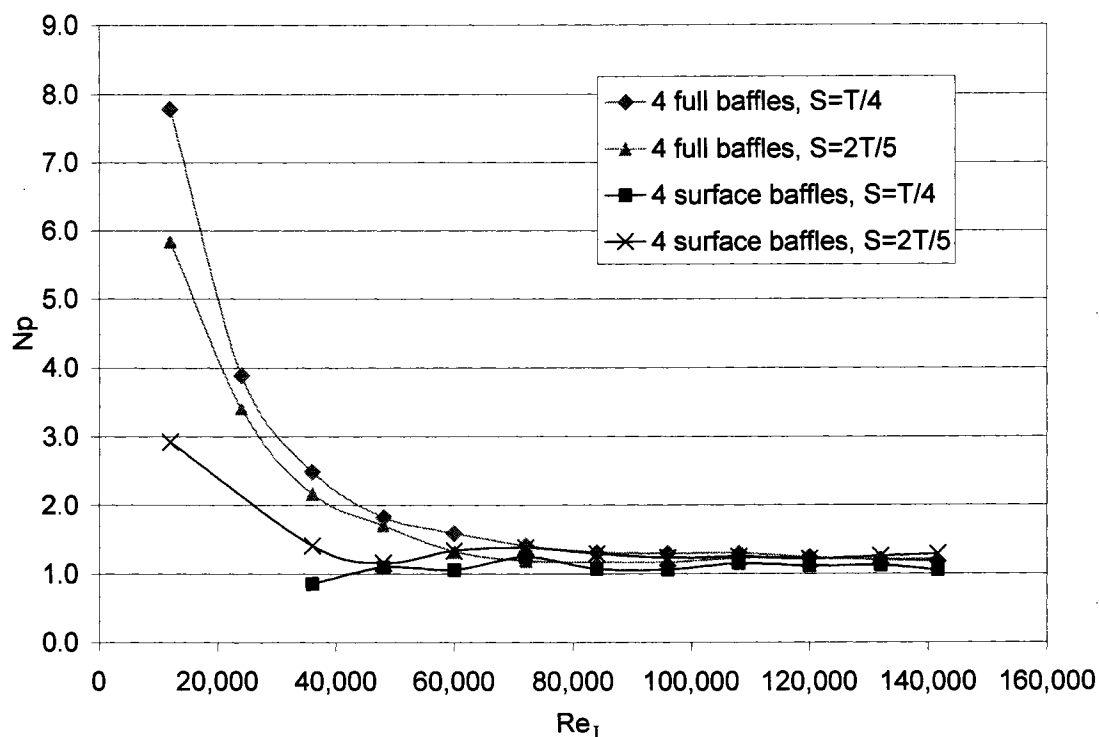
Figure 3.13: Effect of baffle configuration on Np for the PBTU (D = T/3, 2%v/v). Np becomes constant for both configurations once the system is in the fully turbulent flow regime (Re > 60,000).

Moving now to compare the performance of both baffle configurations in terms of power, shown in Figures 3.14 and 3.15, there is a reduction in power consumption when the surface baffle configuration is used. For the T/2 impeller at for large values of submergence, the power consumed drops by a factor of 3, and for the PBTU the different is as large as a factor of 6. Again it is clear that the formation of a secondary loop causes an abrupt increase in power at S/T = 0.33. The surface baffle configuration offers significant savings in terms of power consumption.

51

Figure 3.14: Effect of baffle configuration on P_{jd} for the PBTD and PBTU (D = T/2, 2%v/v). Power consumption drops for both the PBTD and PBTU with the surface baffle configuration.

Figure 3.15 shows the power consumption for the D=T/3 impeller. There is no significant reduction in power when the smaller impeller is used. On the contrary, for the surface baffles the power consumption is higher for the T/3 impeller. The reason for this behavior is the small pumping capacity of the T/3 impeller. The pumping capacity and baffle configuration strongly influence the flow patterns in the tank and these patterns are responsible for creating mean drag and turbulence needed at the surface to achieve efficient solids drawdown.
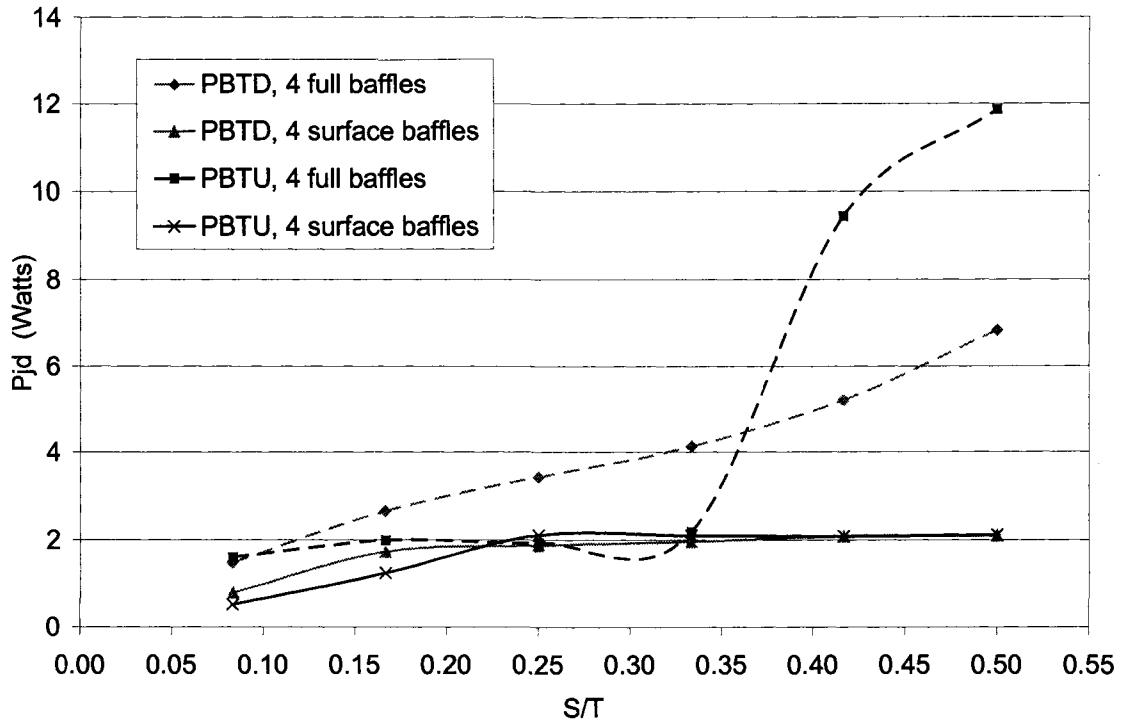
52
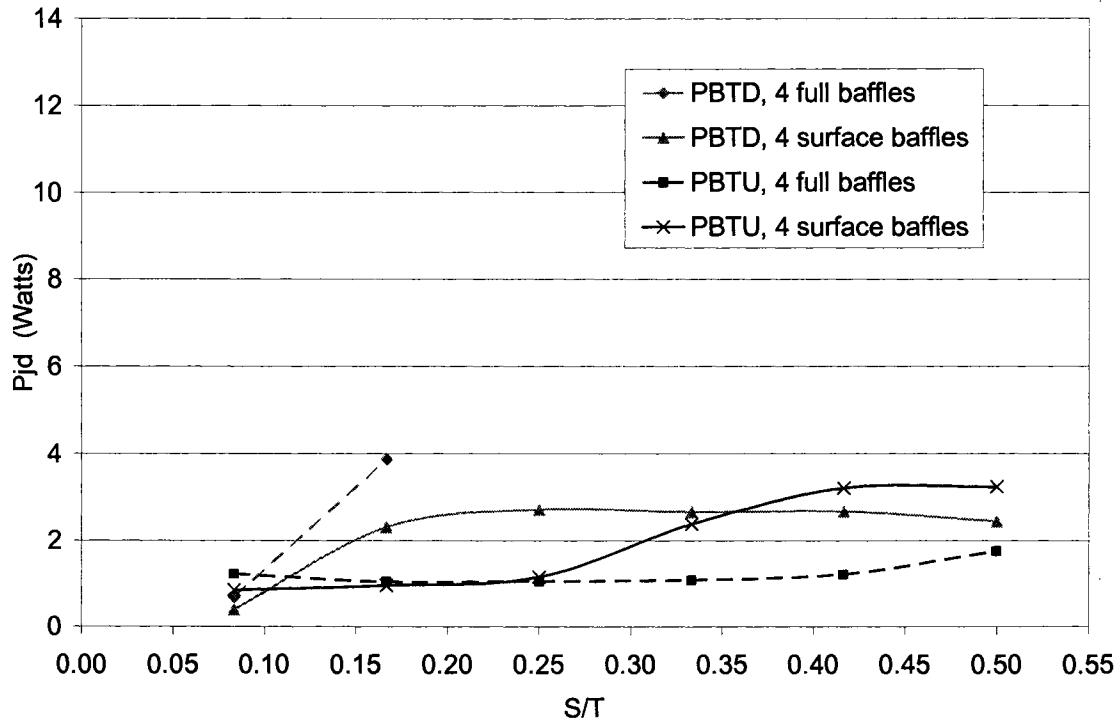
Figure 3.15: Effect of baffle configuration on P_{jd} for the PBTD and PBTU ($D = T/3$, 2%v/v). Power consumption drops for both the PBTD and PBTU with the surface baffle configuration with the exception of the PBTU at large submergences.

3.4.6 Effect of fluid and solids properties

The performance for both the down and up-pumping PBT impellers is sensitive to submergence using the fully baffled configuration, as described in Chapter 2 (Figure 2.14). The same experiment repeated using the surface baffles shows different results. The system is independent of submergence for the PBT impellers as is shown in Figure 3.16. One of the advantages offered by the surface baffle configuration is the turbulent kinetic energy generated by the impeller. This energy is dissipated at the surface for the fully range of submergences studied, in contrast with the fully baffled case where much of the energy is dissipated in the main circulation loop. The surface baffle energy is visible as vigorous mean flow and some vortex formation at the surface. This characteristic of the flow helps the drawdown of particles, and hence smaller values of N_{jd} are obtained even for large values of submergence.

53
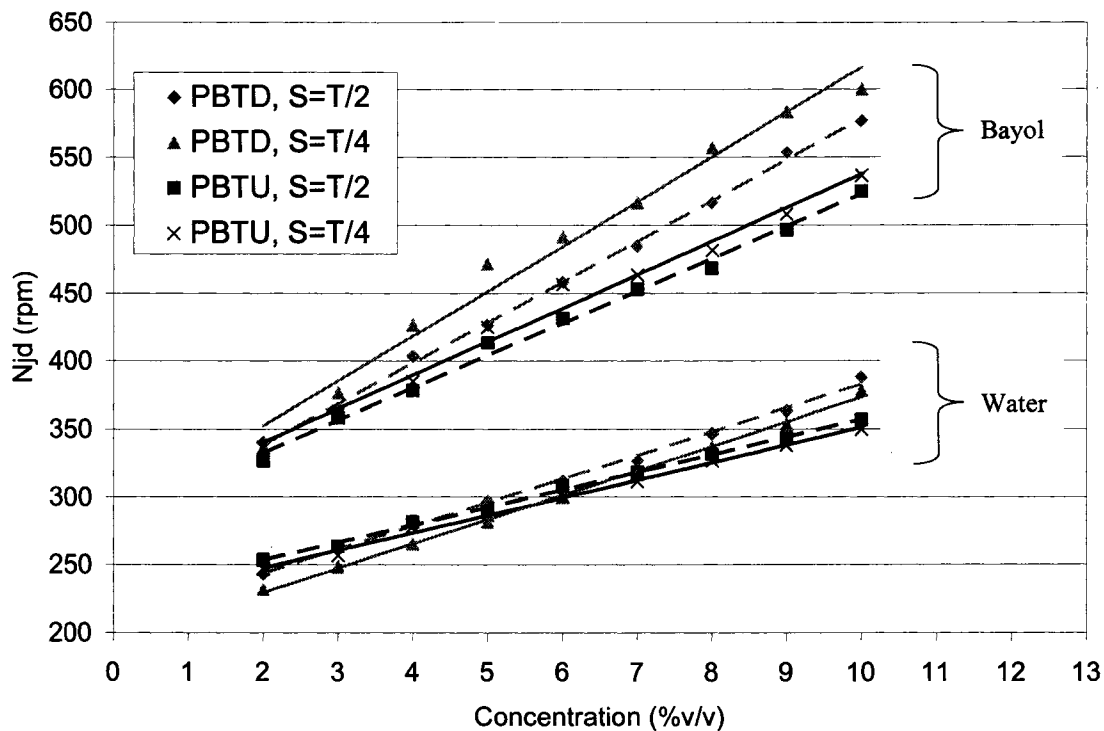
Figure 3.16: Effect of submergence on N_{jd} for the EPS beads 1/ Water and EPS beads 3/Bayol systems (PBTD and PBTU, D = T/2, 4 surface baffles). Note that the 4 surface baffle configuration is not sensitive to submergence, in contrast with the fully baffled case (Figure 2.14).

When using the EPS beads 3/Bayol system, the great quantity of air entering to the system at S=T/4 produces a layer of foam in some zones at the surface (Figure 3.16). This layer tends to retain the particles and is the cause of the larger values of N_{jd} obtained in comparison with the values at S=T/2. This second experiment (EPS beads 3/Bayol system) confirms that the surface baffles minimize the effect of impeller submergence on solids drawdown. As was observed for the fully baffled case, the relationship between N_{jd} and solids concentration is linear.

Comparison of Figures 3.4 and 3.17 shows that the trends for the three different baffle configurations are retained, and even for large values of solids concentration the performance of the surface baffles is more robust than the half-baffles and full baffles.

54

There is, however, a substantial increase in N_{jd} with a higher concentration of solids, as shown in Figure 3.17.
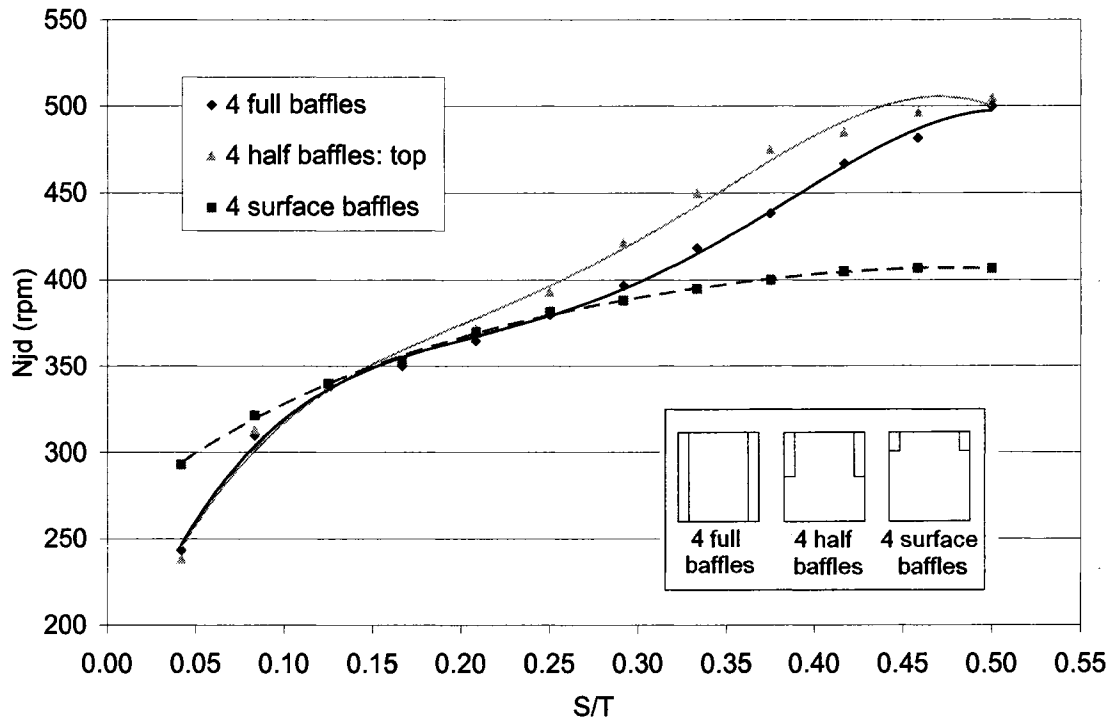
Figure 3.17: Effect of baffle configuration on N_{jd} for the PBTD at high solids fraction (D = T/2, 10%v/v). There is no significant difference in N_{jd} at higher solids loading in comparison with Figure 3.4.

3.5 Concluding remarks

Based on the results obtained the following conclusions can be drawn:

❖ A significant reduction of N_{jd} and more robust performance is obtained with the surface baffles, especially for the PBTU at large values of submergence where the values of N_{jd} become constant in contrast with the sudden increase observed for the fully baffled and half-baffle configurations.

❖ The surface baffle configuration offers a better distribution of solids and a longer circulation time below the surface than the fully baffled and half-baffle configurations, based on visual observations.

❖ The A340 impeller by Lightnin performs per design specification. It is very stable for $S/T<0.3$, and is essentially independent of baffle configuration.

❖ The particle distribution for the A340 is significantly poorer than for the other two impellers.

❖ The four half-baffles offer no advantage over the fully baffled configuration.

❖ None of the up- and down-pumping PBT impellers are sensitive to submergence when surface baffles are used. This is in contrast to the large sensitivity to submergence observed in a fully baffled configuration.

❖ The formation of a foam layer in several zones at the surface prevents particles from being drawdown. The foam layer is more apt to form at low submergences.

❖ The power number measured for the surface baffles configuration is slightly lower (Np=1.24) than for the four fully baffled configuration (Np=1.27).

❖ Reducing the impeller diameter for both the PBTD and PBTU results in higher values of N_{jd} and P_{jd} for most of the configurations studied. A D=T/2 impeller gave the best results.

56

Chapter 4

Conclusions

Solids drawdown mechanisms for floating solids are more complicated than solids suspension mechanisms due to the presence of free surface, or conversely the absence of a fixed wall. The drawdown mechanisms identified in this work are deep vortex formation; drag on the solids due to mean flow, and turbulent eddies of an intermediate size, particularly those that are perpendicular to the surface.

The use of a surface vortex for solids drawdown is not effective, and the surface vortex is not able to distribute solids throughout the tank. Turbulent eddy formation at the surface and mean drag are more efficient mechanisms for solids drawdown, and the distribution of particles in the tank requires the action of strong bulk circulation. This result is contrary to a popular design heuristic which suggests that the use of a surface vortex is effective for solids drawdown. The surface vortex represents an improvement over the nearly stagnant surface observed with single impeller configurations at large submergences, but is a poor solution when the full range of possible configurations is considered.

In tanks in which the formation of a large surface vortex has been suppressed by baffles, high mean velocities and turbulence intensity at the surface are responsible for solids drawdown. The performance of both impellers used (PBTU and PBTD) is sensitive to submergence, and both impellers perform better (lower Njd) when they are closer to the surface. The PBTU is particularly sensitive to submergence, performing much better than the PBTD at small submergences, but worse than the PBTD when the submergence is increased to T/2. When the submergence is less than S/H = 0.375 with the four baffles configuration simulations and experimental results both show that the primary discharge flow reaches the surface of the liquid before it hits the walls. If the submergence is larger than S/H = 0.375 the creation of a secondary loop is observed and much more energy is

57

needed to drawdown the particles. This result will clearly be independent of the size of the tank, and can be considered a firm design guideline.

Computational Fluid Dynamics (CFD) packages for simulations of mixing processes and some other applications are an invaluable tool for expanding our understanding. Data for the surface velocities, turbulence, and flow patterns obtained from CFD simulations helped the understanding of the process and support most of the experimental observations. The values of axial velocity and turbulent kinetic energy obtained from the CFD simulations clearly reveal the main drawdown mechanism at the surface for the different configurations studied. The mean drag mechanism is dominant at large submergences, while for small submergences there is more influence of the turbulent fluctuations mechanism. As expected, an increase in solids concentration requires a bigger intensity of the liquid circulation velocity to achieve complete drawdown of the floating solids.

At the beginning of Chapter 3 the question "How deep the baffles should penetrate into the tank for the new design?" was proposed. Based on the results in this thesis the surface baffles perform better than either half- or fully baffled configurations. The surface baffles create a flow field where all the energy from the impeller is directed towards the surface. This creates high levels of turbulence at the surface which promotes the drawdown of particles. The drawdown mechanisms for this configuration are mean drag and turbulent fluctuations. In addition, the lack of baffles in the lower 80% of the tank promotes tangential flow which gives a better distribution of particles and seems to increase the circulation time of the particles below the surface.

The ability to place the impeller at large submergences without increasing the rotational speed is an advantage of the surface baffles configuration, especially if it is desirable to avoid air entrainment. For both PBTD and PBTU, once the impeller is below the surface baffles the flow patterns and the intensity of mixing are nearly constant as the submergence is increased.

58

The four half-baffles offer no advantage and in some cases perform worse than the fully baffled configuration in terms of both N_{jd} and cloud depth. The half-baffles generate top to bottom circulation, however this circulation is weak and offers really poor distribution of particles in the tank.

When the impeller diameter is reduced from T/2 to T/3 for both the PBTD and PBTU, there is no improvement in the mixing performance. In most cases, the values of N_{jd} and power consumption are higher for the small impeller. The lower pumping capacity of the T/3 impeller is the reason for this behavior. The power number measured for the surface baffle configuration is not significantly different than that measured for the four full baffles configuration for either impeller.

The A340 impeller is the best option for solids drawdown when no more than one baffle can be installed in the tank. The A340 creates the smallest surface vortex in comparison with the PBTD and PBTU impellers for the no baffle or one baffle configuration. However, the performance of the A340 is comparatively poor once the number of baffles is increased to four. The vertical distribution of particles is particularly poor when using the four full baffles or the surface baffles configurations with the A340.

According to this study, surface baffles are the best option for drawdown of floating solids. This novel baffle geometry is one of the first steps toward understanding the drawdown of floating solids. A more extensive characterization of the surface baffles will offer a better understanding of the physics involved for this configuration, and allow a wider range of applications of surface baffles for mixing processes.

Finally, I would like to quote Charles Kettering, "The world hates change, yet it is the only thing that has brought progress."

References

Bakker, A., Frijlink, J.J. (1989). The drawdown and dispersion of floating solids in aerated and unaerated stirred vessels. *Chem Eng Res Des*, 67, 208-210.

Baldi, G., Conti, R., and Alaria, E. (1978). Complete suspension of particles in mechanically agitated vessels. *Chem Eng Sci*, 33, 21.

Bhattacharya, S., Hebert, D., and Kresta, S. (2007). Air Entrainment in baffled stirred tanks. *Chem Eng Res Des,* 85, 654-664.

Bhattacharya, S., Kresta, S. (2002). CFD Simulations of Three-dimensional Wall Jets in a Stirred Tank. *The Canadian Journal of Chemical Engineering*, Vol.80.

Choudhury, N. H. (1997). Improved predictive methods for solids suspension in agitated vessels at high solids loadings. Ph.D. dissertation, University of Arkansas, Fayetteville, AR.

Coy, D., LaRoche, R. and Kresta, S. (1996). Use of Sliding Mesh Simulations to Predict Circulation Patterns in Stirred Tanks. *AIChE Annual Meeting*, Chicago, November 10-15.

Fokema, M., Kresta, S., and Wood, P. E. (1994). Importance of using the correct impeller boundary conditions for CFD simulations of stirred tanks. *Can. J. Chem. Eng.*, 72, 177-183.

Gigas, B. (2005). Lightnin, Pers.Corr.

Hemrajani, R. R., Smith, D. L., Koros, R. M., and Tarmy, B. L. (1988). Suspending floating solids in stirrer tanks: Mixer design, scale-up and optimization. *Proceedings of the sixth European conference on mixing*, 24-26 May, Pavia, Italy.

Joosten, G. E. H., Schilder, J. G. M., and Broere, A. M. (1977). The suspension of floating solids in stirred vessels. *Transactions of the Institute of Chemical Engineers*, 55, 220-222.

Kresta, S., and Wood, P. E. (1993). The flow field produced by a 45 degree Pitched Blade Turbine: Changes in the circulation pattern due to off bottom clearance, *Can. J. Chem. Eng.*, 71, 42-53.

Kuzmanic, N., Ljubicic, B. (2001). Suspension of floating solids with up-pumping pitched blade impellers; mixing time and power characteristics. *Chemical Engineering Journal*, 84, 325-333.

Mak, A. T. C. (1992). Solid-liquid mixing in a mechanically agitated vessels. Ph.D. dissertation. University College-London.

Montante, G., Micale, G., Magelli, F. and Brucato, A. (2001). Experiments and CFD predictions of solid particle distribution in a vessel agitated with four pitched blade turbines. *Trans I ChemE*, 79: 1005–1010.

Nienow, A. W. (1968). Suspension of solids particles in turbine-agitated vessels. *Chem. Eng. Sci.*, 23, 1453.

Nienow, A.W., and W., Bujalski, (2004). The Versatility of Up-pumping Hydrofoil Agitators. *Chem Eng Res Des*, 82, no. A9, 1073-1081

Özcan-Taskin, G., McGrath, C. (2001). Draw down of light particles in stirrer tanks. *Trans I Chem E*, 79(A7), 789-794.

Özcan-Taskin, G., Wei, H. (2003). The effect of impeller-to-tank diameter ratio on draw down of solids. *Chem Eng Sci*, 58, 2011-2022.

Paul, E. L., Atiemo-Obeng, V. A., Kresta, S. (2003). Handbook of Industrial Mixing. 556-559.

Rao, K. S. M. S. R., V. B. Rewatkar, and J. B. Joshi (1988). Critical impeller speed for solid suspension in mechanically agitated contactors. *AIChE J.*, 34(8), 1332.

Siddiqui, H. (1993). Mixing technology for buoyant solids in a nonstandard vessel. *AIChE Journal,*. Vol.39, no 3. 505-509.

Takahashi, K. Sasaki, S. (1999). Complete drawdown and dispersion of floating solids in agitated vessel equipped with ordinary impellers. *Journal of Chemical Engineering of Japan,* Vol. 32, 40-44.

Thring, R. W., Edwards, M. F. (1990). An Experimental Investigation into the Complete Suspension of Floating Solids in an Agitated Tank. *Ind Eng Chem*, Res. 29, 676-682.

Zwietering, T.N. (1958). Suspending of Solids Particles in Liquids by Agitators. *Chem Eng Sci*, 8 (3), 244-253.